PHILOSOPHICAL TRANSACTIONS OF THE ROYAL SOCIETY A MATHEMATICAL, PHYSICAL & ENGINEERING SCIENCES

Field Emission and Field Ionization in Liquid ^{4}He

A. Phillips and P. V. E. McClintock

Phil. Trans. R. Soc. Lond. A 1975 **278**, 271-310
doi: 10.1098/rsta.1975.0026

FIELD EMISSION AND FIELD IONIZATION IN LIQUID ^{4}He

By A. PHILLIPS and P. V. E. McCLINTOCK
Department of Physics, University of Lancaster, Lancaster

(*Communicated by W. F. Vinen, F.R.S. – Received* 16 *September* 1974)

CONTENTS

Spacecharge limited field emission and field ionization currents in liquid ^{4}He have been investigated for emitter potentials V_s, temperatures T, and pressures p in the ranges $0 < |V_s| < 3500\,\mathrm{V}$, $0.3 < T < 5\,\mathrm{K}$, $1 < p < 25 \times 10^5\,\mathrm{Pa}$, respectively. In each case, for constant p and V_s, the current i passes through a maximum at a temperature T_{max} near 1.5 K. For $T > T_{max}$ it is possible to account for the characteristics on the basis of a simple theory which does not require a detailed knowledge of the current generating mechanisms, and which enables values of the ionic mobilities $\mu_\pm$ to be deduced from the data. The rapid decrease in i below T_{max} is ascribed to a process in which ions become trapped on quantized vortices and subsequently escape again. A model is developed to enable values of the ionic escape probabilities to be derived from the experimental results. It was found that the current becomes temperature independent below 0.4 K. The low temperature $i(V_s)$ characteristics suggest that an effective mobility can be defined to describe ionic motion through a self generated vortex tangle. The

negative ion current for $T < 0.9$ K showed a rapid increase with pressure for $p > 10^6$ Pa. This behaviour is ascribed to the presence of an increasing proportion of free ions travelling at the Landau velocity, owing to a decrease with p of the vortex nucleation probability ν; and a model is developed to enable values of ν to be deduced from the experimental data. The conduction mechanism below 0.7 K is discussed, but is not understood in detail. It is inferred that Vinen's F_2 parameter becomes temperature independent below 0.4 K.

1. Introduction

When a large negative potential is applied to a sharp metal point, electrons are able to escape from the metal through field emission, a tunnelling process rendered possible by the intense electric field at its surface. When the emitter is in a vacuum these electrons accelerate rapidly away under the influence of the electric field, which itself remains almost unperturbed by the presence of charge between it and the collecting electrode. Field emission under vacuum conditions is well understood (Gomer 1961).

If, however, the vacuum is replaced by a liquid, the situation becomes very much more complicated. The negative charge carriers, which are now not necessarily electrons (see § 1(*b*)), move much more slowly, their drift velocity being determined by a balance between opposing forces due to the electric field and the drag imposed by the liquid. This smaller velocity of the charge carriers results in the building up of spacecharge which, through its tendency to reduce the field at the emitter, exerts a controlling influence on the magnitude of the emission current. As an additional complication the current generating mechanism may include secondary ionization processes in the liquid close to the emitter, as well as pure field emission.

Field ionization occurs when a large positive potential is applied to the metal point which, in its normal application in the field ion microscope, is surrounded by a gas at low pressure, usually helium. Under these conditions an electron on a gas atom close to the emitter is able to tunnel from the atom into the emitter, leaving behind a positive ion which accelerates away towards the collecting electrode under influence of the electric field. Field ionization in a rarefied gas is well understood (Gomer 1961; Müller & Tsong 1969). As in the case of field emission, however, field ionization phenomena in a liquid are complicated by the influences of spacecharge and of secondary ionization processes.

Field emission and ionization in liquids are important partly because high flux ion sources based on these emission mechanisms are useful in providing the ions required for a variety of experiments to investigate the nature of the liquids concerned. The phenomena are, however, often of considerable interest in their own right, and we shall see that this is particularly true in the case of liquid helium. In this paper we present and discuss the results of a detailed experimental investigation of spacecharge limited field emission and field ionization in liquid ^{4}He at temperatures above 0.3 K and pressures up to the solidification point.

(*a*) *Previous work*

Halpern & Gomer (1965, 1969*a*, *b*) have investigated field emission and ionization processes in a variety of liquids under their saturated vapour pressures, including ^{4}He. McClintock (1969, 1970, 1973*c*), Hickson & McClintock (1970, 1971), McClintock & Read-Forrest (1973) and McClintock, Crowley & Davis (1973) have investigated various aspects of the phenomena in liquid ^{4}He under low pressure. Gavin & McClintock (1973) and Phillips & McClintock (1973) have published some preliminary data regarding field emission and ionization in liquid ^{4}He

under pressures up to the solidification point. Field emission and ionization in liquid ^{3}He under low pressure have been investigated by McClintock (1971, 1973*a*).

Ionic mobilities in liquid ^{4}He under its saturated vapour pressure have been determined from field emission and ionization characteristics by Halpern & Gomer (1969*a*, *b*), Sitton & Moss (1971) and by Gavin & McClintock (1973). McClintock (1972, 1973*b*) has used the emission characteristics to measure mobilities in liquid ^{3}He under low pressure. Blaisse, Goldschvartz & Slagter (1970) have measured mobilities in liquid ^{4}He under its saturated vapour using a different technique, but one based on the large ion fluxes which can be injected by means of field emission and ionization. Phillips & McClintock (1974) have shown that it is possible to deduce values of the rate at which negative ions create vortex rings in He II from field emission characteristics under pressure. Reichert & Dahm (1974) have investigated the spin-polarized electrons which can be field emitted into liquid helium from an iron emission tip.

(*b*) *The charge carriers*

It is known that the charge carriers in liquid helium are not simply electrons and He^+ ions (for a brief review see Donnelly 1967). An electron placed in liquid helium thermalizes in a few picoseconds (Onn & Silver 1969) by creating a charged bubble whose radius r_i is believed to lie in the range $1.0 < r_i < 1.6$ nm, depending on the externally applied pressure. The positive charge carrier, in contrast, is believed to be a small sphere, radius about 0.6 nm, of solid helium electrostrictively solidified by the electric field arising from the positively charged entity, perhaps a molecular ion of the form He_n^+, at its centre. Experiments by Ihas & Sanders (1970) and Ihas (1971) appear to have shown that although the original snowball model of the positive charge carrier proposed by Atkins (1959) may be an oversimplification, his general picture is probably correct. In this paper we shall refer to both types of charge carrier as ions.

Ihas & Sanders (1971) and Ihas (1971) have shown that, in addition to the negative ion described above, there appears to be a large number of other types of negative ion which can be drawn into the liquid from a glow discharge above its surface, and which can be distinguished by their different mobilities. Reichart & Dahm (1974) have shown, however, that these exotic ions are apparently not produced by a field emitter immersed in the liquid, so that there is no need for us to take any further account of them here.

The only other type of charge carrier which one might expect to be present in our experiments is the quantized vortex ring, which is able to carry either a positive or negative charge, and whose dynamic behaviour is very different from that of a free particle (Rayfield & Reif 1964). We shall see, however, that our charge densities and electric fields are of such magnitudes that it is unlikely that individual charged vortex rings will be able to exist in the cell for more than a small fraction of the ionic transit time.

(*c*) *Theory of field emission and ionization in liquid helium*

Halpern & Gomer (1969*a*) have developed a simple analysis which enables spacecharge limited discharges in liquids, initiated by field emission or ionization, to be understood without a detailed knowledge of the actual generating mechanisms; and a brief discussion of these ideas, in relation particularly to liquid helium, has been presented in an earlier paper (McClintock 1973*a*). In the present paper, therefore, we will indicate briefly the underlying physical principles, and then simply quote the relevant equations which emerge from the analysis. Apart from any complications which may arise from secondary ionization processes, the actual emission

PHILOSOPHICAL TRANSACTIONS OF THE ROYAL SOCIETY A MATHEMATICAL, PHYSICAL & ENGINEERING SCIENCES

mechanisms in a liquid are likely to be exactly the same as they are in the case of a vacuum or of a rarified gas, for field emission or ionization respectively: we discuss this point in more detail in §1 (*d*). The magnitude of the emitted current is likely in each case therefore to be a very rapid function of the electric field at the source which, for currents greater than about 10^{-9} A, is itself controlled principally by the spacecharge formed at large radii. Thus, while the emission currents $< 10^{-9}$ A will be determined directly by the physical nature of the generating mechanism, investigations at higher currents may be expected to yield mainly information about the behaviour of ions in liquid helium under electric fields of a few kilovolts per centimetre. We shall be concerned purely with the latter situation in the present paper.

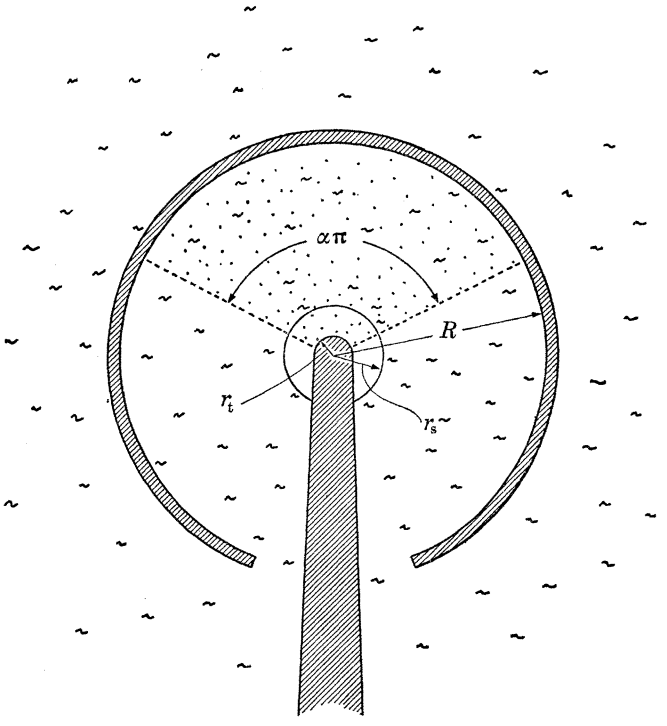

FIGURE 1. Idealized spherical geometry used in discussing the theory of field emission and field ionization in liquid helium. The radius of curvature r_s of the source region is not necessarily identical with that r_t of the emitter; but r_s, $r_t \ll R$, where R is the radius of the collecting electrode. The emission is assumed confined to a cone of solid angle $\alpha\pi$ sr.

To calculate the magnitude of the emission current it is necessary to solve the Poisson equation

$$\nabla^2 V = -\rho/\epsilon\epsilon_0, \tag{1}$$

where V is the potential, ρ the charge density, ϵ the dielectric constant and ϵ_0 the permittivity of free space, subject to appropriate boundary conditions. We assume, as illustrated in figure 1, overall spherical symmetry with a source of radius r_s and a collecting electrode of radius R, but we suppose the emission is restricted to a solid angle of $\alpha\pi$ sr. As boundary conditions we take: $V = V_s$ at $r = r_s$ and $V = 0$ at $r = R$; and $dV/dr = F_s$ at $r = r_s$. The latter condition amounts to the assumption that, since i is an exceedingly rapid function of electric field, the field at the source can be regarded as remaining effectively constant over the whole range of currents which we investigate. The charge density,

$$\rho = i/\alpha\pi r^2 v, \tag{2}$$

where i is the total current and v is the ionic drift velocity at radius r, so that, before a solution of the Poisson equation can be attempted, it is necessary to make some assumptions about the behaviour of v.

It is perhaps most natural to assume that $v = \mu \mathrm{d}V/\mathrm{d}r$, where μ is thus defined as the ionic mobility. In this case (1) may be integrated to give

$$\mathrm{d}V/\mathrm{d}r = 1.548 \times 10^5 (i/\alpha\epsilon\mu r)^{\frac{1}{2}}, \tag{3}$$

for $r \gg r_s$, and

$$V_s = V_0 + 3.097 \times 10^5 (Ri/\alpha\epsilon\mu)^{\frac{1}{2}}, \tag{4}$$

in the fully spacecharge dominated regime. Here, V_s and $V_0 = F_s r_s$ are in volts, r and R are in metres, i is in amperes, and μ is in $\mathrm{m^2\,V^{-1}\,s^{-1}}$.

If, on the other hand, the ionic drift velocity has a constant value independent of electric field, which might for example be the case in He II if the ions were limited to the Landau critical velocity for roton creation, then the equations corresponding to (3) and (4) are

$$\mathrm{d}V/\mathrm{d}r = 3.595 \times 10^{10}\, i/\alpha\epsilon v r, \tag{5}$$

for $r \gg r_s$, and

$$V_s = V_0 + 3.595 \times 10^{10}\, i[\ln(R/r_s) - 1]/\alpha\epsilon v, \tag{6}$$

in the fully spacecharge dominated regime.

These two cases constitute the extremes of behaviour to be expected under normal circumstances: there will usually be *some* increase in ionic drift velocity when the electric field is increased, even although the increase may not always be describable in terms of a constant mobility. It is interesting to note that, for fixed V_s, (4) and (6) imply $i \propto \mu$ and $i \propto v$ respectively. Thus, looking now at (3) and (5), it is clear that in either case the profile of the electric field, and hence also that of the charge density, in the cell will remain constant even for large changes in i caused by changes in the values of μ or v respectively.

(*d*) *The current generating mechanisms*

It seems clear that not all of the ions arriving at the collector are produced by pure field emission or ionization, although the discharges are almost certainly initiated by these processes.

The negative ion current in the spacecharge limited regime is noisy, and upon subsequent microscopic examination it is found that the emitter has been blunted. Both these observations suggest the presence of secondary ionization processes in an unstable vapour bubble surrounding the emitter, since the consequent bombardment of the metal surface by heavy positive ions would account for the blunting. This conclusion is also supported by the fact that in liquid helium under its saturated vapour pressure, an emitting tip can be seen apparently glowing dull red, with the appearance of a point source of the same colour as a helium discharge lamp. Reichert & Dahm (1974) have shown, nonetheless, through their experiments on spin-polarized electrons, that a significant fraction of the negative ions arriving at the collector enter the liquid as field emitted electrons.

At much lower currents, where the discharge does not appear to be spacecharge limited, the negative ion current is extremely stable and varies linearly with emitter potential. This curious behaviour has been observed in both liquid ^{4}He (Halpern & Gomer 1969*a*) and in liquid ^{3}He (McClintock 1973*a*), but its origin is not yet understood.

In the case of the positive ion current, two distinct generating mechanisms have been distinguished, depending on the magnitude of the current. For $i \lesssim 10^{-8}$ A the current is associated

with the presence of a vapour bubble enveloping the emitter. In contrast to the field emission case, however, it appears that the bubble is stable since the current does not normally exhibit any low frequency noise. Again, there is emission of light, but no blunting occurs, which is not surprising because bombardment of the emitter by the relatively much lighter electrons would not be expected to result in damage. When positive ion emission of *ca.* 10^{-6} A occurs in He II under its saturated vapour pressure and there are only a few cm of liquid above the emitter, the bubble becomes readily visible through a low powered microscope as a sphere reaching about 0.1 mm in diameter. At lower currents the bubble shrinks and appears to conform more closely to the shape of the emitter. Henson (1970) reported oscillations of the positive ion current at frequencies of a few tens of kilohertz and while we have also observed this phenomenon on several occasions we do not understand the mechanism which is responsible.

When with a reduction in V_s or μ the positive ion current falls below *ca.* 10^{-8} A one of two things can happen: either the discharge extinguishes completely; or the current exhibits a discontinuous drop, or a noisy regime, leading to a lower regime of stable behaviour as the current falls a little further. It seems (McClintock 1973*a*) that the former behaviour is characteristic of a relatively blunt emitter, or one that has been smoothed by field evaporation. The lower regime seems for experiments at low pressure to be associated with emitters which have not undergone any smoothing process and have not been used for field emission in the liquid, and it is therefore possible that the emission is occurring from the sharp excrescences which probably exist on a virgin emission tip which has been prepared by the drop-in-loop method (Müller & Tsong 1969). Currents in the lower regime vary roughly exponentially with emitter potential down to the lowest values which have been measured, and probably arise from pure field ionization. Owing to the electrostrictive pressure of the high local electric field a layer of solid helium will be formed around the emitter. Electrons tunnel into the metal tip from atoms in the solid and the resultant positive charges have to diffuse to the solid–liquid interface before travelling as positive ions to the collector. A careful study of currents generated in the lower regime might, therefore, yield interesting information concerning, for example, the electronic band structure of solid helium (Halpern & Gomer 1969*b*), but the present work is confined to a study of spacecharge limited currents.

An interesting feature of both positive and negative currents is that the value of α is usually found to be about 2.5 – very much larger than the value of about 0.6 which is usually obtained in the cases of field emission or ionization in a vacuum or rarefied gas. The angular distribution of the emitted current was investigated experimentally by McClintock & Read-Forrest (1973), who found that the current density emitted at right angles to the emitter was usually larger than that in the axial direction, a typical result being that plotted as a symmetrical polar histogram in figure 2. A detailed explanation of this behaviour has not been given, but there appear to be two possible mechanisms which may be involved. Emission in the transverse direction may perhaps be almost entirely due to secondary ionization processes in a vapour bubble and, if this bubble envelopes a significant length of the shank of the emitter, then the transverse emission would be anomalously large. If this explanation of the current distribution is correct, then the axial emission from a ferromagnetic emitter should contain a higher proportion of spin polarized electrons than the transverse emission, but Reichert & Dahm (1974) do not appear to have searched for such an effect. The other possibility is that charge spreading out of the initial emission cone, which was ignored in deriving equations (3)–(6), may after all be important, although this seems somewhat less likely.

Whatever the origin of the angular distribution of the current, it is important to bear in mind

that the α which enters our equations is some averaged value which cannot be predicted in advance, but must be determined by experiment through use of equations (4) or (6) in conjunction with characteristics obtained under circumstances where the ionic mobility or velocity is known. It is believed that the observed small systematic deviations from equation (4) are the result of changes in the effective value of α (McClintock 1973*a*).

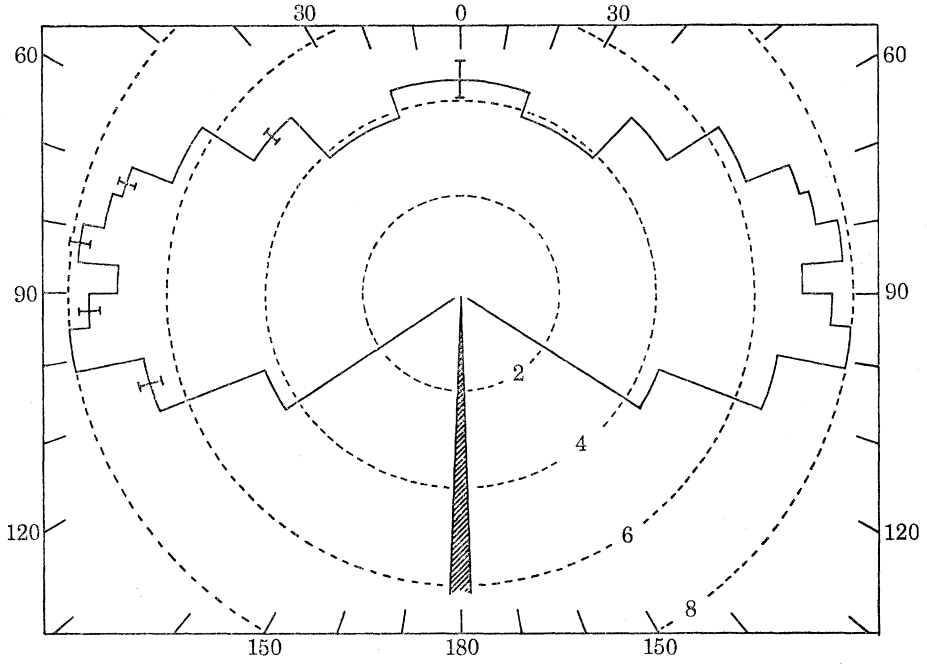

FIGURE 2. Angular distribution of the negative ion current emitted into liquid helium at 1.52 K under s.v.p. from an emitter at -3000 V. The current density, plotted radially, is in 10^{-11} A mm^{-2}.

2. APPARATUS AND EXPERIMENTAL PROCEDURE

The tungsten emitters were prepared by electrochemical etching as described previously (McClintock 1973*a*), and were mounted 3 mm from the closed end of a cylindrical brass collector of i.d. 10 mm. The copper experimental chamber was designed to work at pressures of up to 25×10^5 Pa (1 bar = 10^5 Pa) and was tested initially to 40×10^5 Pa at room temperature. The chamber was closed by means of two circular brass end pieces, each of which was provided with metal–glass seals for electrical leads, and which were sealed in position with indium 'O' rings. The electrode structure was mounted on one of these end pieces, and the other was used to support a 470 Ω Speer carbon resistance thermometer. The chamber was mounted in a ^{3}He refrigerator of conventional design, able to reach a temperature of 0.25 K in the absence of the thermal heat load imposed by the experiment.

The experimental sample of ^{4}He was obtained from a standard high pressure cylinder which stored the gas at a pressure of up to 130×10^5 Pa and which was fitted with a regulator able to deliver gas in the pressure range $0–40 \times 10^5$ Pa. The pressure was measured by means of an absolute pressure bourdon gauge (Wallace & Tiernan type FA233) calibrated $0–35 \times 10^5$ Pa (0–35 bar). The gas was cleaned by passing it over charcoal at liquid nitrogen temperature and then passed into the cryostat through a 0.5 mm i.d. cupronickel capillary tube in which it condensed in thermal contact with the main (4.2 K) liquid helium bath. The 0.5 mm capillary

was also thermally anchored to the 1.1 K bath, and then admitted the sample to a 600 mm length of 0.13 mm i.d. stainless steel capillary, coiled in a helix, which conveyed the sample to the experimental chamber. Under these conditions the sample could be cooled to just below 0.3 K.

The carbon thermometer was calibrated against ^{3}He vapour pressure above 0.5 K and, after fitting the data to a suitable empirical relation, the calibration was then extrapolated to 0.3 K. It is estimated that the errors introduced by the extrapolation procedure would not have been more than 20 mK at 0.3 K; and since, as will be shown in § 3, the emission current is almost independent of temperature below 0.5 K, small errors in thermometry will not be important in this range.

In practice the presence of the capillary tube made it impossible to pump all the air from the chamber, and it was therefore removed by a flushing procedure: the chamber was pressurized to 5×10^5 Pa with clean ^{4}He gas which had passed through the cleaners; it was then pumped out for about 30 min at which time the pressure was estimated to have fallen to about 1 k Pa; and the whole process was repeated three times. No trouble was experienced with blocked capillaries provided that this procedure was followed.

Up to 3100 V could be applied to the emitter from a Keithley model 246 stabilized power supply, and the emission currents were measured with a Keithley model 602 electrometer coupled to a chart recorder, as described previously (McClintock 1973*a*) in the case of liquid ^{3}He. When, as in § 3 (*b*), voltages in excess of 3100 V were required, a Brandenburg model 507R stabilized 0–5 kV supply was available.

At our lowest temperatures the thermal capacity of the ^{4}He sample is lower by a factor of 2000 than that of the ^{3}He sample in the earlier work, with the consequent danger of a significant temperature rise in the sample during the measuring period. In the present case it may be shown that, on the time scale of the measurements, the thermal load due to the measuring current is thrown straight on to the refrigerator ^{3}He bath, which may be regarded as remaining effectively at a constant temperature. The difference ΔT in the temperatures of the sample during and immediately prior to the measurement must therefore be the sum of the two Kapitza temperature discontinuities between sample and chamber, and ^{3}He and refrigerator pot. We have calculated that for our worst case ($V_s = 3500$ V, $p = 25 \times 10^5$ Pa, $T = 0.3$ K) $\Delta T \simeq 56$ mK, and that under more typical operating conditions ($V_s = 2000$ V, $p = 15 \times 10^5$ Pa, $T = 0.4$ K) $\Delta T \simeq 1$ mK. These estimates are consistent with the transient behaviour of the carbon thermometer in the chamber, and showed that no serious errors would result from the procedure in which we took for T its value immediately before the measurement.

Since it had been observed that emitters became blunted when used for field emission in liquid helium, all the field ionization measurements for any particular tip were carried out before those involving field emission. As an additional precaution, it was decided somewhat arbitrarily to ensure that the current was never allowed to exceed 1 μA in the case of positive ions, and 0.7 μA in the case of negative ions. Used in this way, the emitters appeared to enjoy a long life and, in fact, all the measurements described in § 3 were made with the same emitter, involving numerous experimental runs with liquid helium over a period of 5 months.

3. Experimental results

In this section we present a selection of our experimental results, reserving a detailed discussion of their significance to §4. The raw data were typically as shown in figure 3, the conditions under which they were recorded being shown in table 1. The currents were usually noisy, the extent of the low frequency fluctuations most often being in the region of $\pm 2\,\%$ of the average value. Although negative ion currents in the spacecharge regime invariably displayed some noise, the positive ion emission frequently appeared to be completely stable over a wide range of currents (figure 3*a*, *c*, *d*, *e*). In cases where $\mathrm{d}i/\mathrm{d}T$ was so large that the small change in T caused by the direct heating effect of the emission current resulted in a significant gradient $\mathrm{d}i/\mathrm{d}t$ during the measuring period (figure 3*c*, *d*, *g*, *h*), the recorder plots were extrapolated back to the moment at which the emitter was switched on.

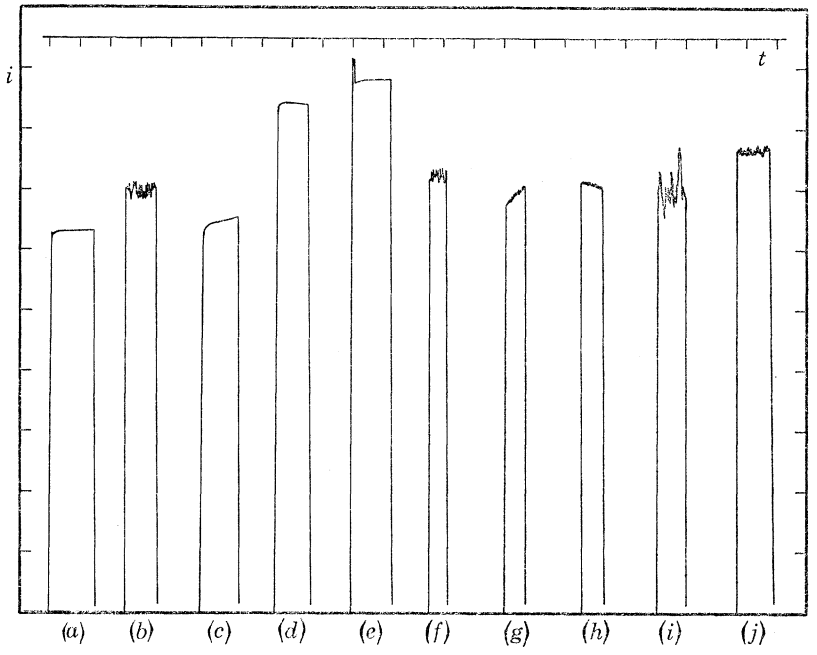

Figure 3. Examples of raw data, traced directly from the $Y(t)$ recorder output in each case. Traces (*a*)–(*e*) refer to field ionization; (*f*)–(*j*) refer to field emission; the conditions under which the data were recorded, and the time and current scales in each case, are specified in table 1.

Table 1. Experimental conditions under which the traces shown in figure 3 were recorded

trace	emitter potential / V	temperature / K	pressure / 10^5 Pa	time per scale division / s	current per scale division / A
(*a*)	+3000	3.56	25	10	10^{-8}
(*b*)	+3000	3.56	1	10	3×10^{-8}
(*c*)	+3000	0.88	24	5	10^{-8}
(*d*)	+3000	1.38	24	10	3×10^{-8}
(*e*)	+1500	0.94	8	10	3×10^{-10}
(*f*)	−2500	0.30	10	10	3×10^{-9}
(*g*)	−3000	1.29	1	10	10^{-8}
(*h*)	−3000	1.68	1	10	3×10^{-8}
(*i*)	−1200	3.87	15	5	10^{-9}
(*j*)	−3000	0.81	25	2.5	3×10^{-8}

PHILOSOPHICAL TRANSACTIONS OF THE ROYAL SOCIETY A MATHEMATICAL, PHYSICAL & ENGINEERING SCIENCES

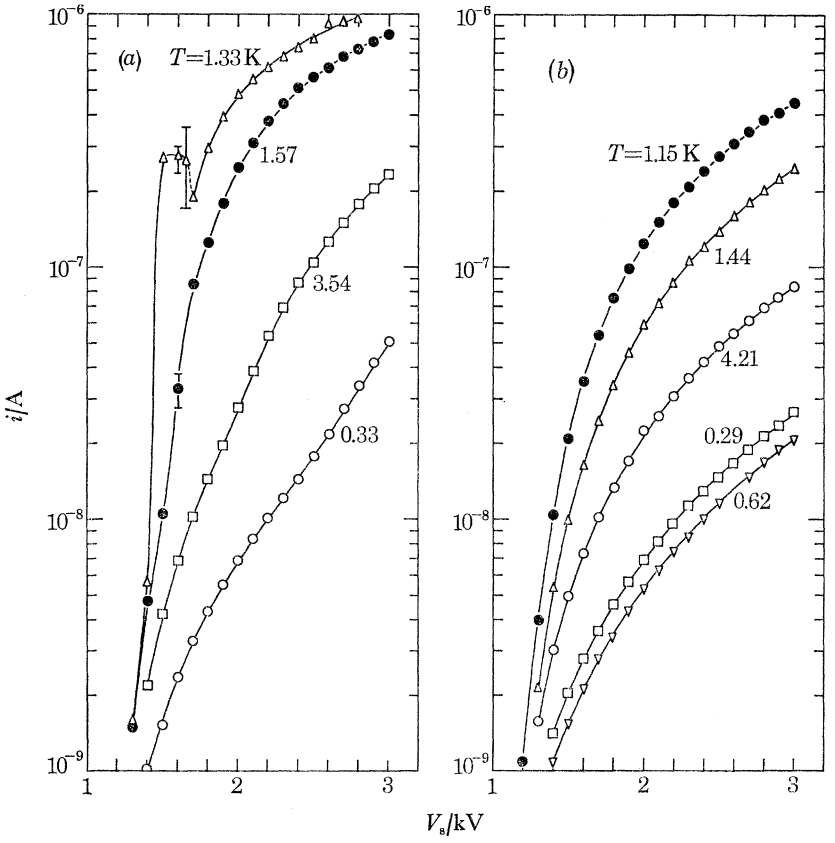

FIGURE 4. Field ionization current i as a function of emitter potential V_s at various temperatures: (a) under pressure of 10^5 Pa ; and (b) under 24×10^5 Pa

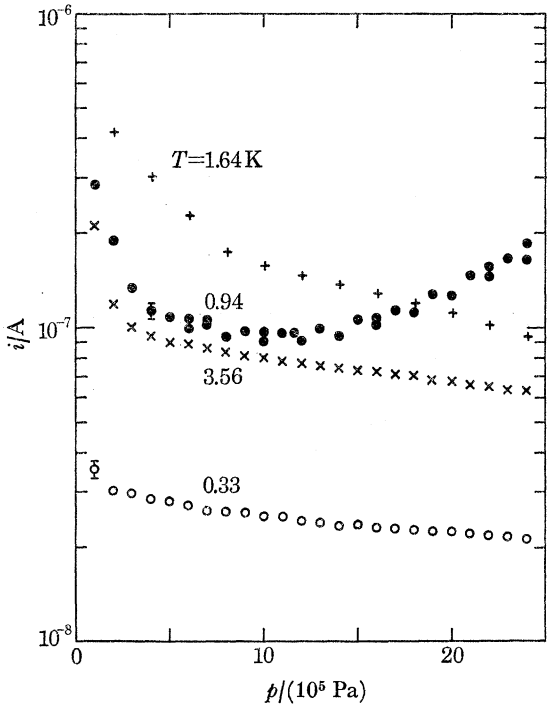

FIGURE 5. Field ionization current i as a function of pressure p at various temperatures and with an emitter potential $V_s = 3000$ V.

For the sake of clarity we will present separately in §3(*a*) and §3(*b*) experimental results relating respectively to field ionization and field emission: it will be taken as understood that, for field emission, numerical values given for V_s and V_0 are of negative sign. In figures 4–12 noise in the currents was smaller than the size of the symbols, except where otherwise indicated by means of error bars.

(*a*) *Field ionization data*

Current–voltage characteristics were measured at pressures $p = 1, 5, 10, 20$ and 24×10^5 Pa, typical results being as shown in figure 4. Currents at 10^5 Pa tended to be noisy and were sometimes unstable (figure 4*a*), but these effects diminished rapidly as the pressure was increased. The characteristics for all $p > 5 \times 10^5$ Pa were very similar to those for 24×10^5 Pa (figure 4*b*).

The effect of pressure on the currents was also measured directly and, except in the temperature range close to 1 K, a relatively weak negative dependence was usually observed (figure 5). At the lowest pressures and highest currents, however, the currents were again noisy, unstable,

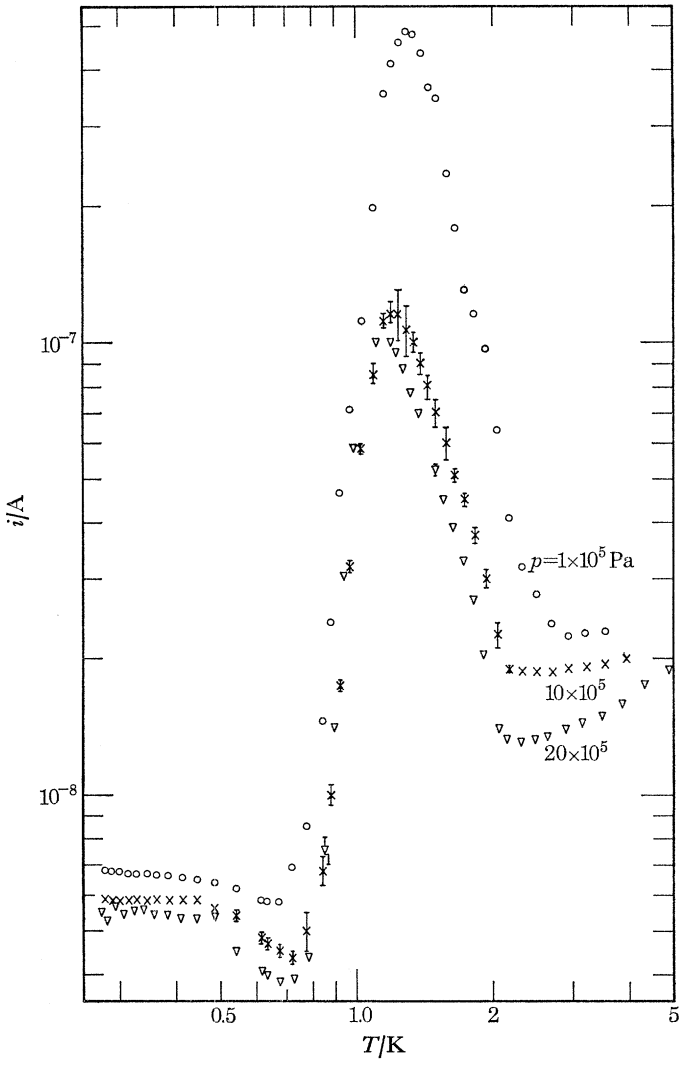

FIGURE 6. Field ionization current i as a function of temperature T at three pressures p and with an emitter potential $V_s = 2000$ V.

and somewhat larger than would have been expected on the basis of a back extrapolation from the data at higher pressures.

Current–temperature characteristics were measured in the range $0.3 < T < 4$ K for $p = 1$, 5, 10, 15, 20 and 24×10^5 Pa, and using a number of different emitter potentials between 1500 and 3000 V. Typical results are shown in figures 6 and 7. The curves are very similar in shape to those reported earlier (Hickson & McClintock 1970), but with the important difference that the

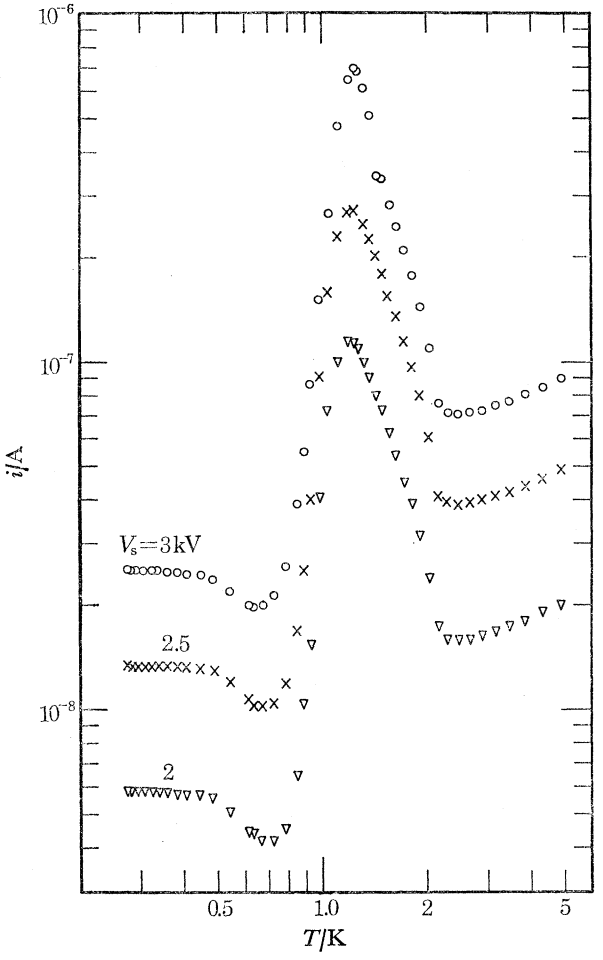

FIGURE 7. Field ionization current i as a function of temperature T at three emitter potentials V_s and under a pressure of $p = 15 \times 10^5$ Pa.

currents do not extinguish in the temperature range just below 1 K. An interesting feature (figure 6) is the way in which the 2000 V, 10^5 Pa, curve seems to break away from the other two as the temperature is reduced below 2 K, and then almost rejoins them below 0.6 K. It appears that the maximum in the current occurs at a temperature which is weakly dependent on the pressure, moving from 1.30 ± 0.02 K at 10^5 Pa to 1.11 ± 0.02 K at 24×10^5 Pa, in the case of the 2000 V data. There is perhaps a suggestion (figure 7) that the temperature of the maximum may increase very slightly with increasing emitter potential but the effect, if it exists, is smaller than the estimated uncertainties in our measurements.

The data were reproducible within experimental error except to the extent that, sometimes, cycling to room temperature and back again resulted in all the currents being reduced by about

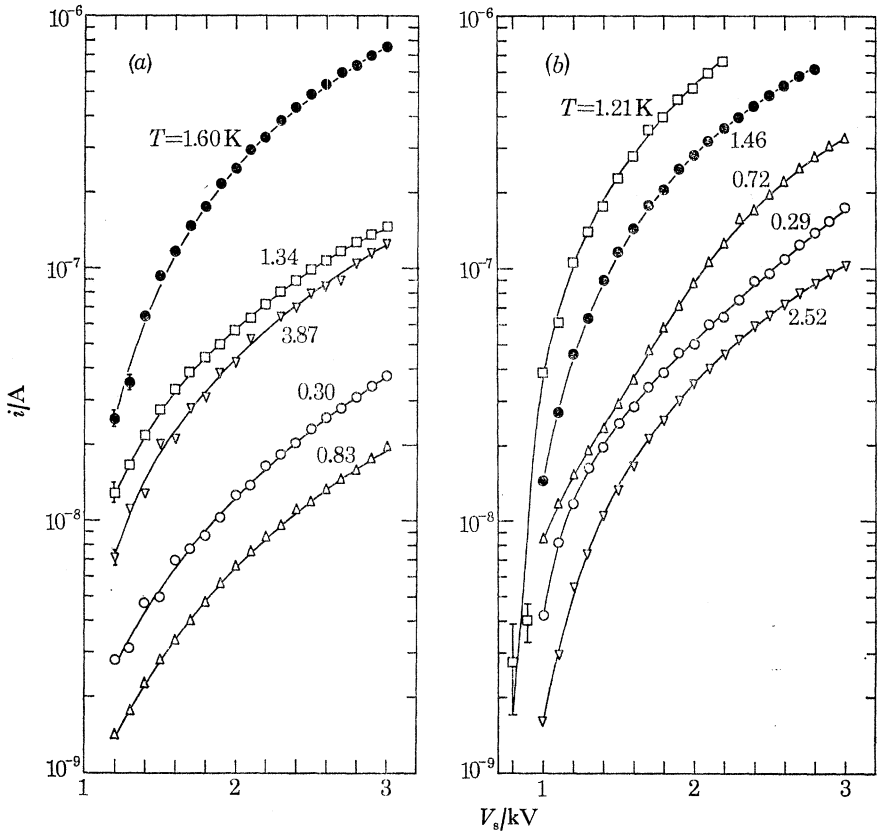

FIGURE 8. Field emission current i as a function of emitter potential V_s at various temperatures: (a) under a pressure of $p = 10^5$ Pa; and (b) under $p = 25 \times 10^5$ Pa.

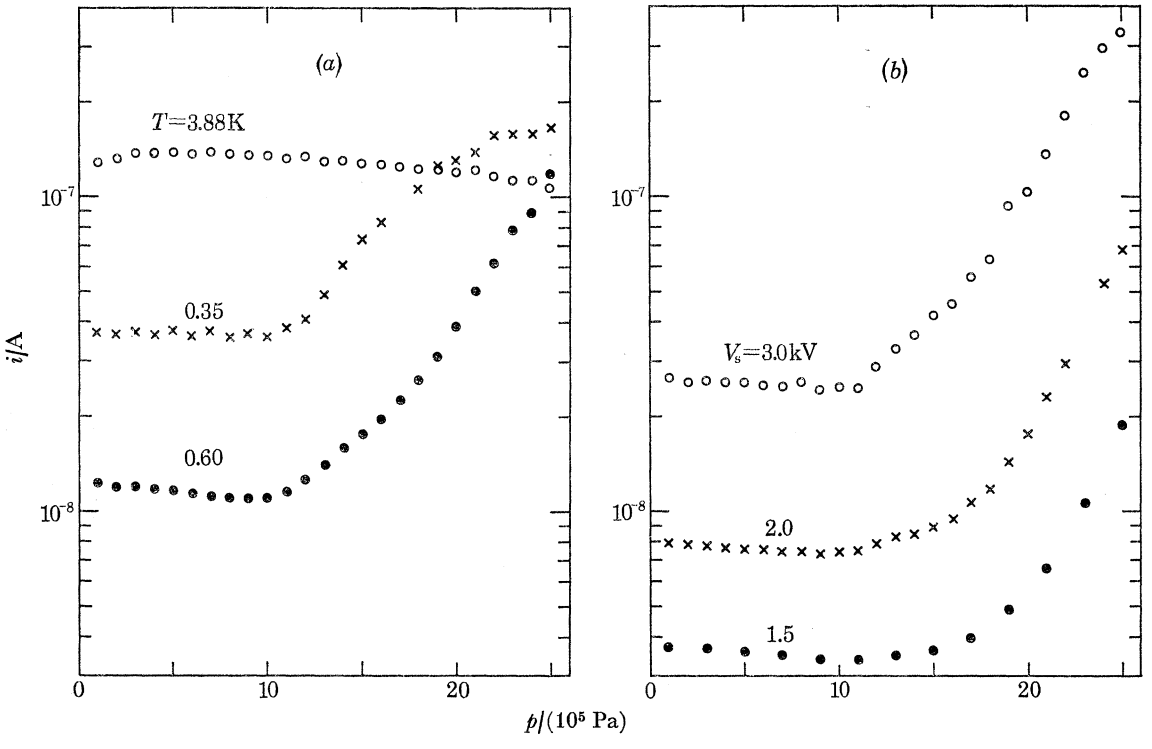

FIGURE 9. Field emission current i as a function of pressure p: (a) at three temperatures T with an emitter potential $V_s = 3.0$ kV; and (b) with three emitter potentials V_s, at a temperature $T = 0.71$ K.

8 %. It was particularly on account of this phenomenon that we recorded directly a number of current–pressure characteristics, in addition to those for current–voltage and current–temperature at a variety of fixed pressures.

(*b*) *Field emission data*

The current–voltage curves (figure 8) are somewhat similar to those for field ionization, but the currents did not display any particularly noisy or unstable regions at low pressure. The 25×10^5 Pa characteristics below 0.9 K, however, appear to exhibit anomalous behaviour: the 0.29 K and 0.72 K curves seem inconsistent in general shape with those for higher temperatures, or with any of those at 10^5 Pa.

It is immediately apparent from current–pressure plots (figure 9) that this behaviour was associated with a rapid increase of current with pressure above about 12×10^5 Pa for temperatures below 1 K. The magnitude of this increase, and the detailed shape of the characteristic, were dependent on the emitter potential (figure 9*b*). No such behaviour was found at higher temperatures where a weak negative dependence on pressure was observed above 10×10^5 Pa (figure 9*a*, 3.88 K curve).

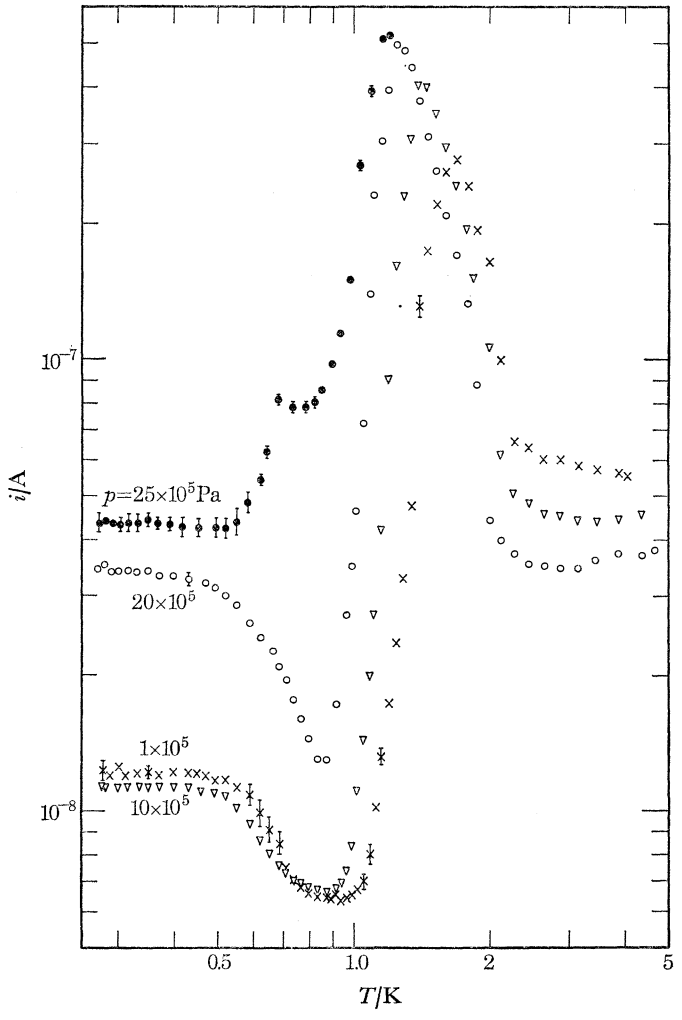

FIGURE 10. Field emission current i as a function of temperature at various pressures p and with an emitter potential of V_s = 2000 V.

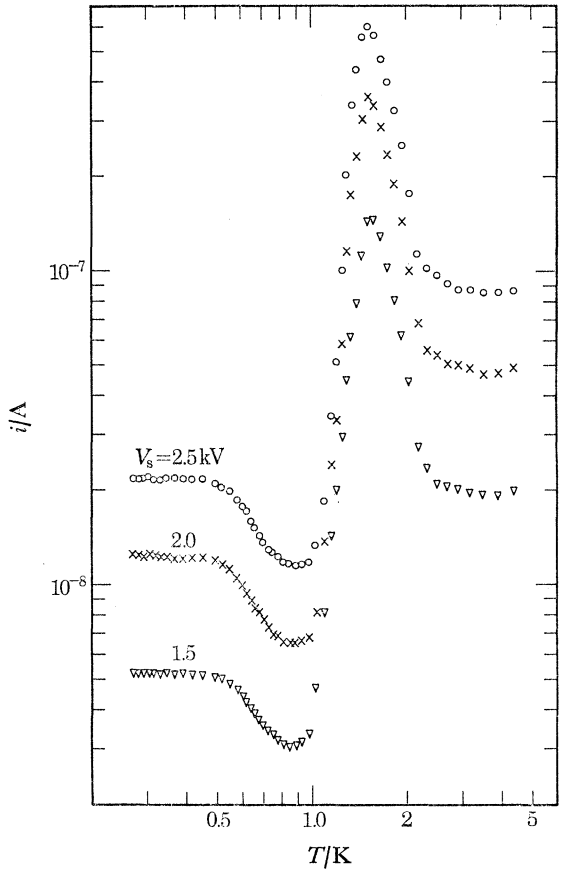

FIGURE 11. Field emission current i as a function of temperature T at three different emitter potentials V_s under pressure $p = 5 \times 10^5$ Pa.

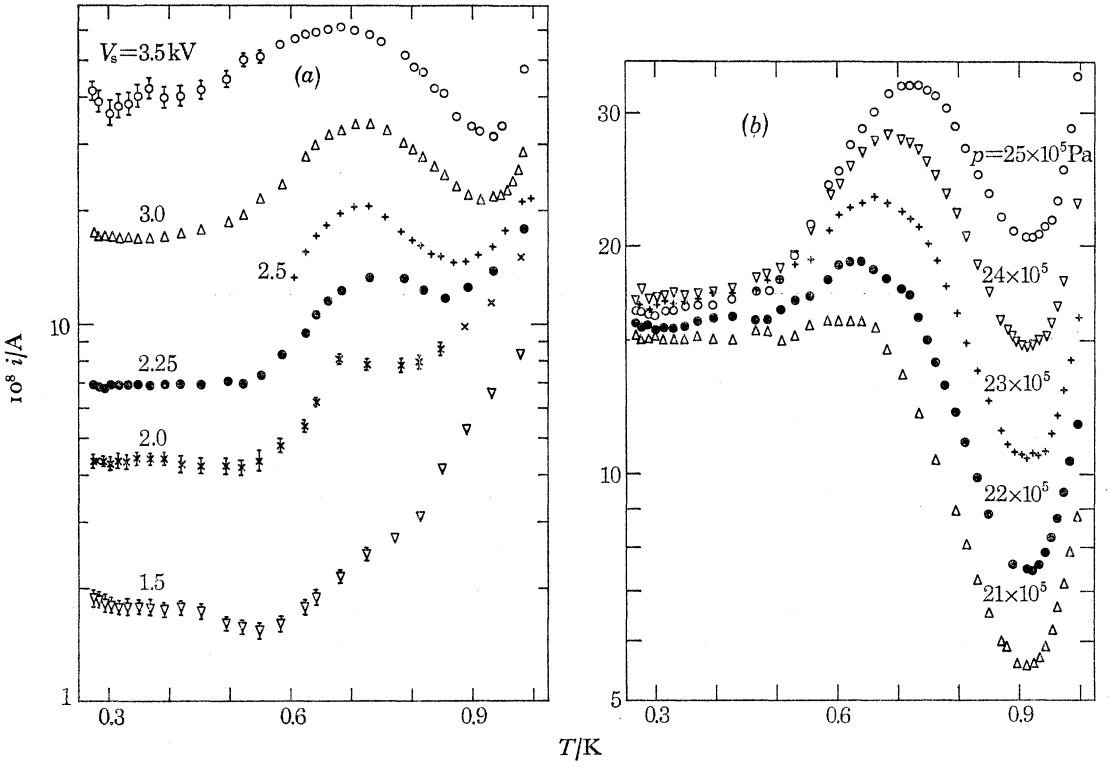

FIGURE 12. Field emission current i under high pressure as a function of temperature T below 1 K: (a) at various emitter potentials V_s under pressure $p = 25 \times 10^5$ Pa and (b) under various pressures p with emitter potential $V_s = 3000$ V.

The pressure dependence of the current is also readily apparent in the current–temperature curves below 1 K, which are completely different in the case of pressures above and below 10×10^5 Pa (figure 10). Below 10×10^5 Pa the characteristic is very similar to that observed for field ionization, except that the minimum in the current below 1 K is deeper. As the pressure is increased above 10×10^5 Pa the whole characteristic below 1 K rises, with the current minimum becoming at first relatively more pronounced and then less so due to the appearance of a small subsidiary maximum in the current near 0.7 K. The temperature of the principal maximum in the current shows a relatively strong pressure dependence, compared to the case of field ionization, moving from 1.67 ± 0.02 K at 10^5 Pa to 1.18 ± 0.02 K at 25×10^5 Pa for an emitter potential of 2000 V. The position of the maximum is almost independent of emitter potential but, if anything, appears to move down in temperature by about 0.03 K as the potential is raised from 1500–2500 V in the case of, for example, data at 5×10^5 Pa (figure 11).

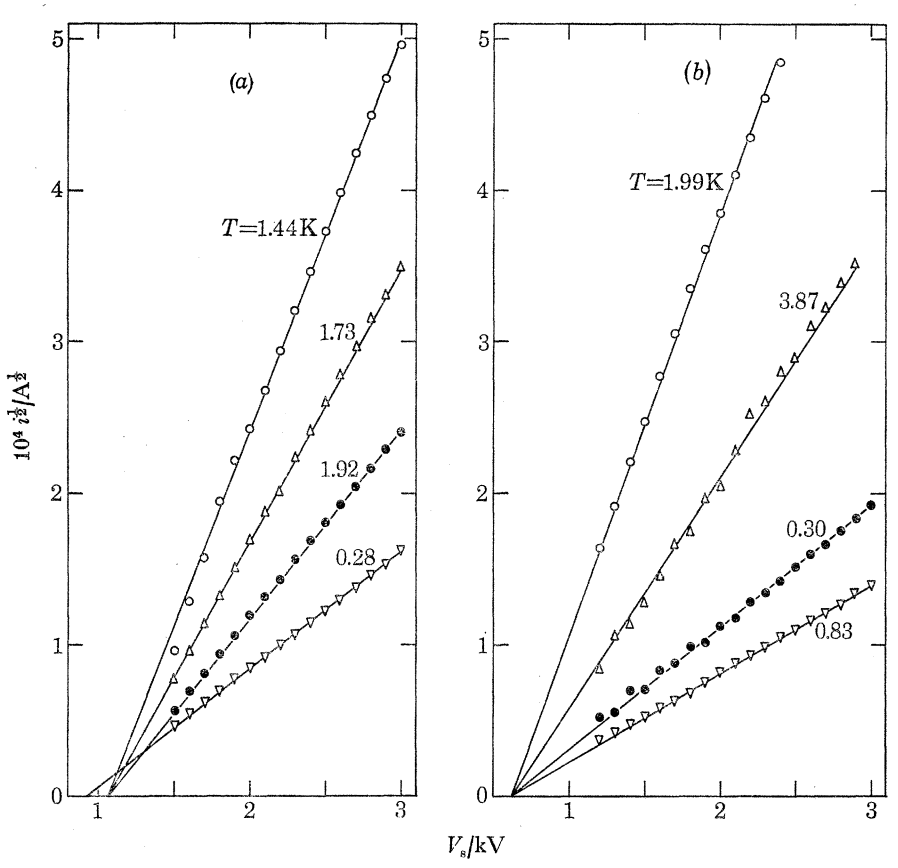

FIGURE 13. Comparison of experimental data with equation (4). (Current $i)^{\frac{1}{2}}$ is plotted against emitter potential V_s at various temperatures: (*a*) for field ionization under pressure $p = 24 \times 10^5$ Pa; (*b*) for field emission under pressure $p = 10^5$ Pa. The straight lines have been drawn by eye through the data.

We have also investigated in more detail the small subsidiary current maximum which occurs near 0.7 K. Its size and shape are strongly dependent on both emitter potential (figure 12*a*) and pressure (figure 12*b*).

Field emission currents were more reproducible than those generated by field ionization provided that, on cooling down and filling the sample chamber, the emitter was run for about 10 min continuously at its maximum current 7×10^{-7} A before any data were recorded. Because of

bombardment by positive ions, this procedure would have ensured that any oxide layer or other extraneous material was removed, leaving a clean tungsten surface for use during measurement of the characteristics.

4. Discussion of experimental results

Because the data presented in the previous section refer to situations where the magnitude of the emission is controlled by spacecharge, the observed dependences of the current on temperature, pressure and emitter potential must be ascribed to corresponding changes with T, p and V_s in the way that ions move through the liquid. At temperatures above those at which the principal maxima in the currents occur, the charge carriers are all bare ions whose drift velocities are proportional to the electric field so that the analysis leading to equation (4) above is applicable in a straightforward manner. We discuss those of our results which fall into these temperature ranges, and derive values of the ionic mobility by fitting our results to this equation, in §4 (*a*).

At temperatures below those of the principal current maxima the situation appears to be greatly complicated by trapping of the ions on quantized vortices in the superfluid. We consider in §4 (*b*) how this mechanism can account for the general shape of the $i(p, T)$ characteristics.

In many cases the current arriving at the collector has apparently been carried across the chamber in the form of a mixture of bare ions and charged vortices, and its magnitude is, in general, likely to depend both on the probability ν per unit time that an ion will nucleate a vortex ring, and also on the probability P that a vortex borne ion will escape. A full theoretical analysis of this situation would clearly be exceedingly difficult and we therefore confine ourselves to a detailed consideration of two extreme situations where, on the basis of certain simplifying assumptions, we can construct models capable of accounting for the principal features of the observed phenomena. In §4 (*c*) we consider the situation where ν is so large that the time spent as a bare ion after leaving the emitter is negligible, and we show how values of P may then be derived from our data; and in §4 (*d*) we show that for temperatures at which P is so small that thermally activated escapes can be ignored, it is possible to deduce values of ν. In §4 (*e*) we present a brief speculative discussion of the conduction mechanism in the low temperature limit.

(*a*) *Ionic mobilities*

Where conduction is by bare ions and occurs under fully spacecharge dominated conditions, which should be the situation for $i > 10^{-9}$ A at temperatures above the principal current maxima, we expect the characteristics to be described by equation (4). Plots of $i^{\frac{1}{2}}$ against V_s ought therefore to yield straight lines and, except for field ionization under low pressures, we find that this is indeed the case within experimental error (figure 13).

The anomalous behaviour of the positive ion current under low pressures may be attributed to a mixed ion generating mechanism at the source: the heat generated locally may be sufficient to initiate a vapour bubble at the source, but insufficient to sustain it against the external pressure. Under these circumstances one would expect, as is observed, a very noisy current whose average value is larger than that which would be appropriate to generation through pure field ionization, with the bubble forming, collapsing and reforming. The situation is much clearer under saturated vapour pressure (s.v.p.) than at 10^5 Pa. In figure 14 we show some data obtained in another cryostat under s.v.p. (Hickson 1971), and the two generating mechanisms may be distinguished by the different values of the intercepts. (The different gradients may relate to different values of α, which one would not necessarily expect to be the same for the two generating mechanisms.)

PHILOSOPHICAL TRANSACTIONS OF THE ROYAL SOCIETY A MATHEMATICAL, PHYSICAL & ENGINEERING SCIENCES

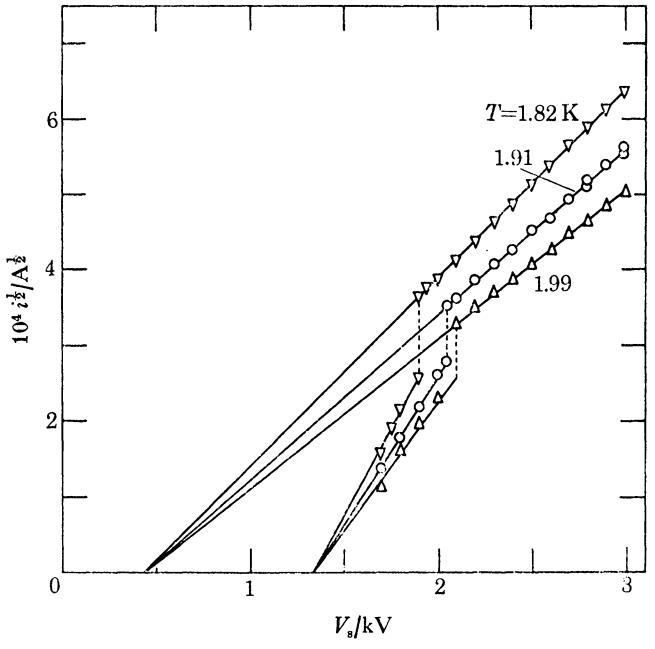

FIGURE 14. Field ionization characteristics under s.v.p.: (current $i)^{\frac{1}{2}}$ is plotted against emitter potential V_s for three temperatures T (after Hickson 1971). The transition from pure field ionization below $i^{\frac{1}{2}} \approx 2.5 \times 10^{-4}\, A^{\frac{1}{2}}$ to emission from a vapour bubble at higher currents is clearly visible.

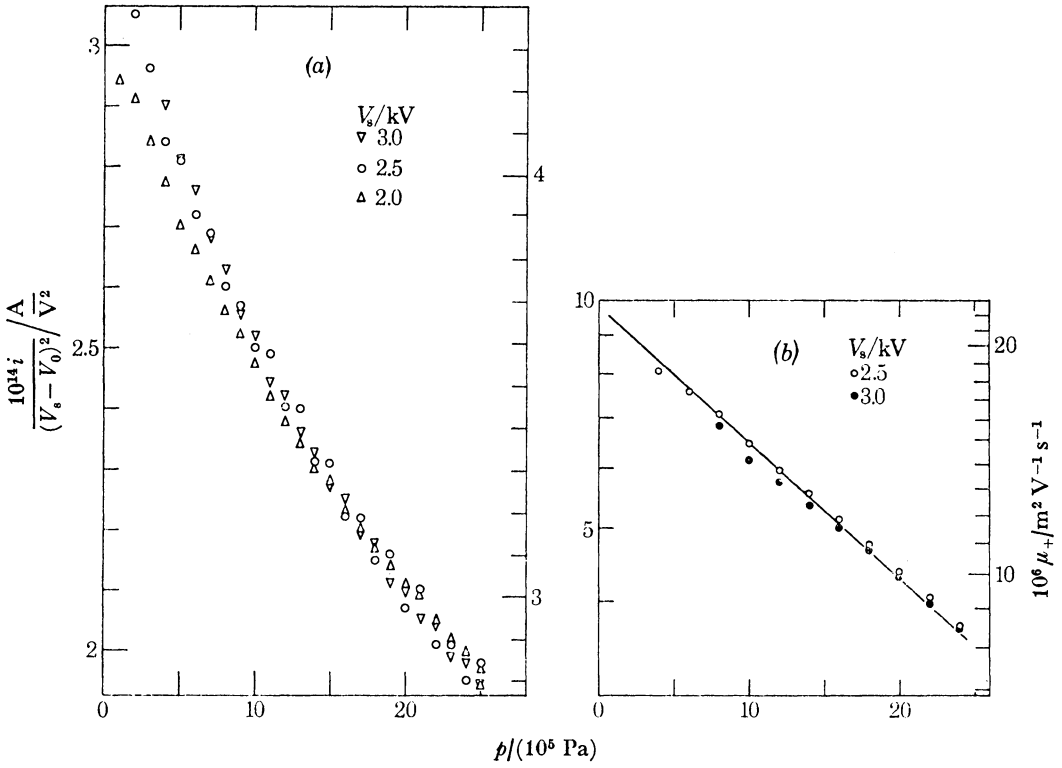

FIGURE 15. Use of (7) to determine positive ion mobility μ_+ as a function of pressure p. The quantity $i/(V_s - V_0)^2$ is proportional to μ_+, is independent of V_s, and has been plotted for various values of V_s using the left hand ordinate scales: (*a*) at 3.56 K; and (*b*) at 1.64 K. The mobility scales on the right hand ordinates have been constructed in each case by extrapolatng the data to s.v.p. and comparing with Schwarz's (1972) measurement of μ_+ at s.v.p. for the same temperature.

Under s.v.p. the transition from one regime to the other is sharp, although marked by some hysteresis, in contrast to the situation at 10^5 Pa where it seems that the current moves steadily, though noisily between the two regimes, as the emitter potential is increased or decreased. This phenomenon provides an explanation (1) for the noisy and peculiarly shaped current–voltage characteristics of figure 4*a*, (2) of the anomalously large currents at 10^5 Pa, $0.6 < T < 2$ K, shown in figure 6 and (3) of the erratic behaviour sometimes observed in earlier experiments (Hickson & McClintock 1970). In connexion with the latter work, we can now understand why the positive ion emission was found to be extinguished completely near 1 K: the emitter in use was probably too blunt to sustain lower regime emission under the experimental conditions being used.

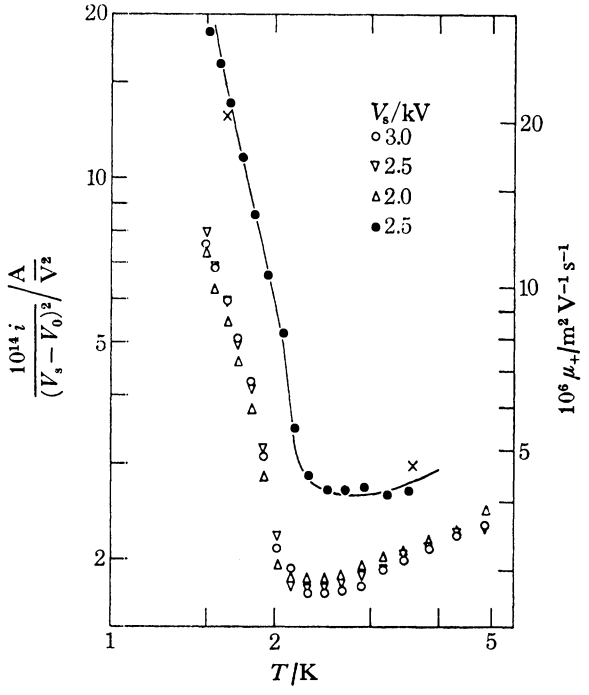

FIGURE 16. Use of (7) to determine positive ion mobility μ_+ as a function of temperature T at pressure $p = 20 \times 10^5$ Pa (open symbols). For details of the procedure used in constructing the figure, see text.

We conclude, therefore, that initiation of the positive discharge is always through field ionization, that under low pressure a vapour bubble which may or may not be stable will form around the emitter and act as a secondary ion source, but that for $p > 5 \times 10^5$ Pa a bubble does not form with the values of V_s used in these experiments, so that the generating mechanism remains purely that of field ionization.

If we assume that α in (4) remains constant within each emission regime even though we do not know its absolute value, then the relative change of ionic mobility with pressure or temperature may be obtained by measuring the gradients of a number of plots such as those of figure 13. A more convenient procedure, however, is simply to measure the changes in current at fixed emitter potential while the pressure or temperature are varied. Rearranging (4) as

$$i/(V_s - V_0)^2 = [\alpha\epsilon/9.59 \times 10^{10} R]\,\mu, \qquad (7)$$

we see that plotting $i/(V_s - V_0)^2$, rather than i, aganst p or T should result in data taken at different emitter potentials falling on the same universal curve which will itself be proportional to the

mobility. This procedure has the advantage that the observed small systematic deviations of the data points on either side of the straight lines of figure 13 will appear as a scatter in the values of $i/(V_s - V_0)^2$, thus providing an estimate of the precision of the measurements.

Figure 15 shows the result of applying this procedure to our current–pressure field ionization data at two temperatures. In order to find the mobility as a function of pressure we need to know the absolute value of the mobility at one pressure. We have used Schwarz's (1972) measurements to fix the point at s.v.p. in each case, extrapolating our curves down to below 10^5 Pa (where, in reality, the current would have become anomalously high owing to the onset of emission from a vapour bubble), thus determining the mobility scales shown on the right hand sides of the two graphs. The straight line in figure 15*b* represents the pressure dependence observed at the same temperature by Meyer & Reif (1961), attributable to changes with p of the roton energy, and the data agree within our experimental uncertainty of about $\pm 4\,\%$.

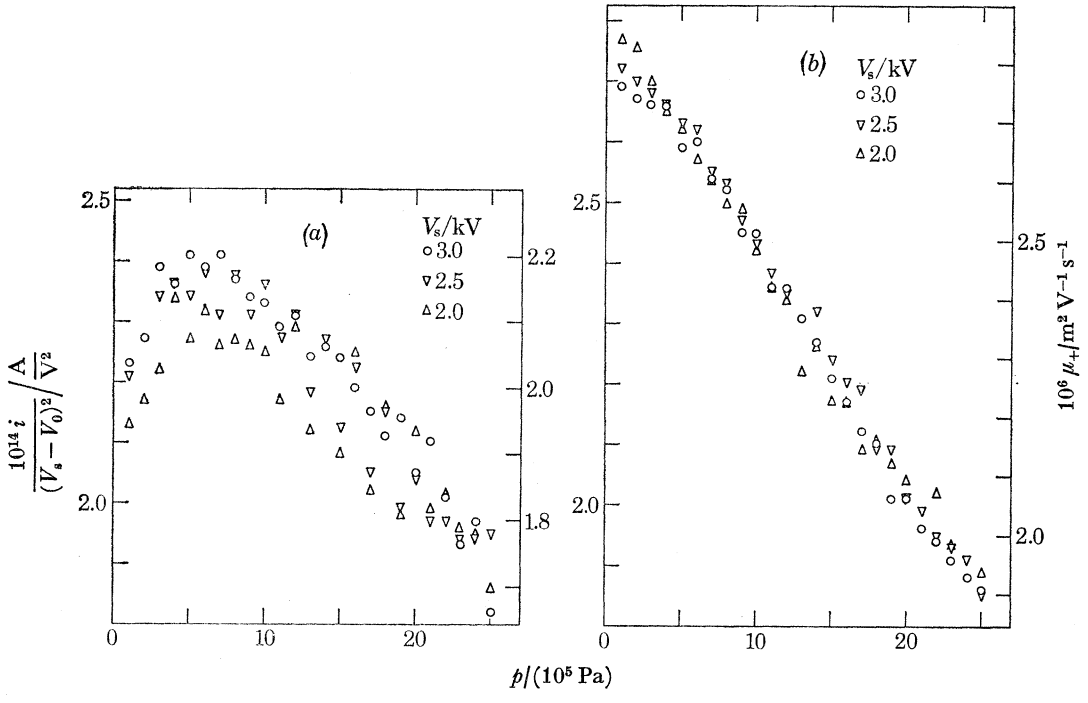

FIGURE 17. Use of (7) to determine negative ion mobility μ_- as a function of pressure p: (*a*) at 3.88 K; and (*b*) 2.35 K. The right hand ordinate scales, giving absolute values of μ_-, have been constructed by comparing the low pressure data with Schwarz's (1972) measurements of μ_- at s.v.p.

A plot of $i/(V_s - V_0)^2$ against T for three emitter potentials at 20×10^5 Pa is shown by the points forming the lower curve of figure 16. Because no high precision mobility measurements other than at s.v.p. appear to have been published, and our data at 10^5 Pa are in the bubble emission regime, we have had to use an indirect procedure to establish an absolute scale for the relative mobility changes represented by this curve. We have used the results of figure 15 to establish what would have been the values of $i/(V_s - V_0)^2$ at s.v.p. for pure field ionization, if bubble formation had not occurred, giving the two points marked X at 1.64 and 3.56 K. We have then superimposed Schwarz's s.v.p. mobility–temperature curve (the solid line) with its associated absolute mobility scale, to fit as accurately as possible through these points. We estimate the accuracy of the 20×10^5 Pa mobility data, obtained in this rather indirect manner, as being about $\pm 10\,\%$.

The filled circles represent the variation of the field ionization current with temperature at 10^5 Pa, 2500 V, scaled so as to bring it into approximate coincidence with Schwarz's curve, in order to show that the agreement is satisfactory. Because these latter data refer to emission from a vapour bubble, and not to pure field ionization, they are quite unrelated to the left hand ordinate scale in $i/(V_s - V_0)^2$.

In the case of field emission, there is no reason to suppose that the ion generating mechanism changes with pressure. The raw current data look very similar at all pressures, and show no obvious discontinuities even under s.v.p. In figure 17 we have plotted $i/(V_s - V_0)^2$ against pressure at two temperatures, for three different emitter potentials in each case. The absolute mobility scales on the right hand side of each graph were constructed as before, by fixing the s.v.p. point in each case to agree with Schwarz's measurements. The precision may be estimated from the scatter of the data points.

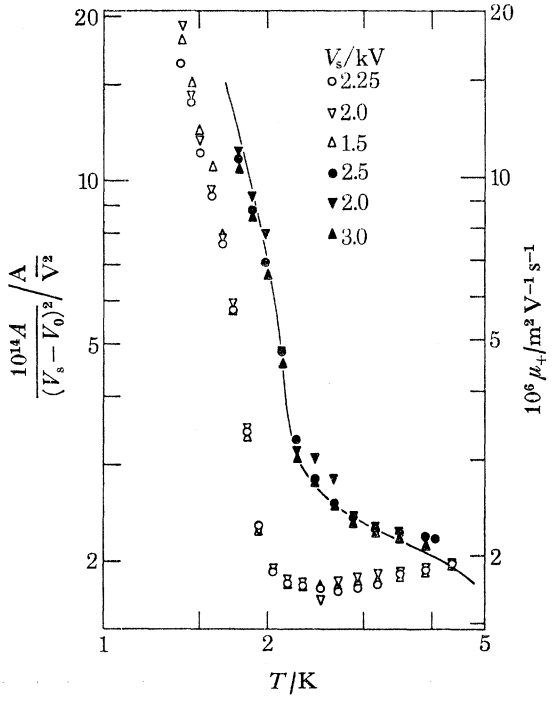

FIGURE 18. Use of (7) to determine negative ion mobility μ_- as a function of temperature T at pressure $p = 25 \times 10^5$ Pa (open symbols). For details of the procedure used in constructing the figure, see text.

In figure 18 we plot $i/(V_s - V_0)^2$ against T at 10^5 and 25×10^5 Pa, for three emitter potentials in each case. The solid line, representing Schwarz's s.v.p. measurements has been positioned, together with its associated mobility scale, so as to pass through the 10^5 Pa data, thus calibrating the 25×10^5 Pa measurements. We may estimate the accuracy of the latter as being approximately the sum of the average scatter in the points on each of the two curves, or about $\pm 7\,\%$.

Using our data to derive mobilities in this way depends on the assumption that the emission angle α is independent of pressure and temperature. There is considerable circumstantial evidence that this is indeed so, at least to a good approximation. In particular, we note that wherever it has been possible to compare our measurements with those made using other techniques, such as in figures 15*b*, 16 and 18, the agreement is satisfactory. Earlier work in liquid ^{3}He (McClintock

1973*b*), where the emission processes are probably identical, also yielded values of $\mu(T)$ in excellent agreement with measurements made by other techniques.

It is interesting to note that, whereas plots of $i^{\frac{1}{2}}$ against V_s at temperatures just below those of the principal current maxima yield gentle curves, data plotted for lower temperatures again produce straight lines with the same intercept, in the case of field emission (figure 13*b*), or almost the same intercept, in the case of field ionization (figure 13*a*). This surprising result suggests that the conduction process in the low temperature limit can again be described, at least to a good approximation, by an effective mobility. In figure 19 we plot $i/(V_s - V_0)^2$ against T for this temperature range for both positive and negative ions at one pressure. The right hand ordinate scales have been constructed by comparison with our high temperature $i/(V_s - V_0)^2$ data, for which the corresponding mobilities have already been deduced above. The *ca.* 12% decrease in $V_0 = F_s r_s$ for field ionization (figure 13*a*) may perhaps be related to a breakdown of our assumption that the electric field at the source remains constant regardless of the magnitude of current being drawn: we have noted some evidence that V_0 increases slightly with mobility at temperatures above the current maximum.

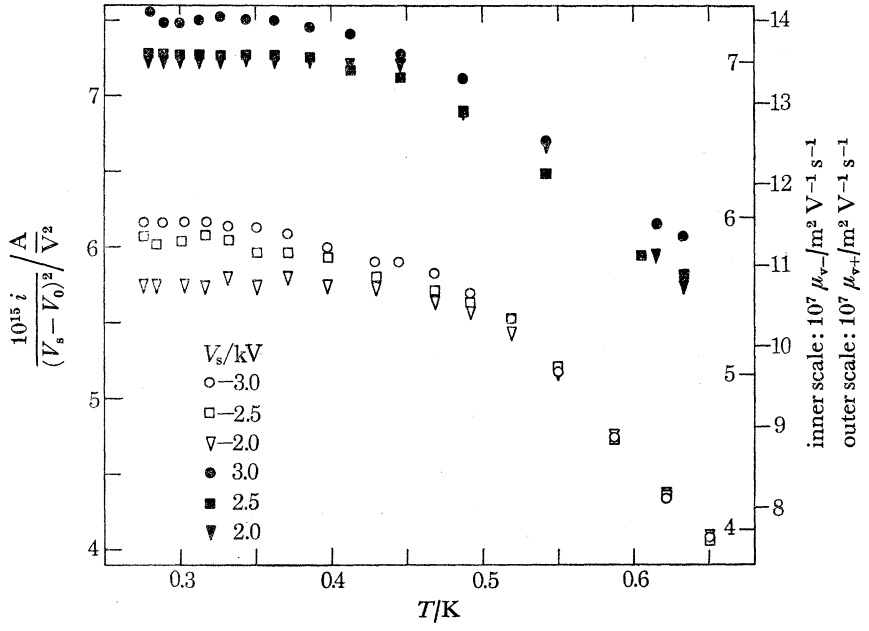

FIGURE 19. Use of (7) to determine vortex limited effective mobilities μ_{v-} and μ_{v+} for negative and positive ions respectively as functions of temperature under a pressure of 10×10^5 Pa.

(*b*) *The influence of vortices*

When an ion is drawn through He II by means of an applied electric field there is a finite probability that it will create and become trapped on a quantized vortex ring (Donnelly & Roberts 1971). The transition rate ν from bare ion to charged vortex ring rises rapidly with the ionic drift velocity v until, at a few tens of metres per second, ν^{-1} becomes comparable with the transit time across a typical experimental cell, and substantial numbers of charged rings arrive at the collector. In fact, ν is such a fast function of v that for any given temperature and pressure it is possible to define an effective critical electric field F_c below which the proportion of vortex rings arriving at the collector will be negligible, and above which only a negligible number of

bare ions reach the collector. Zoll & Schwarz (1973) have measured ν directly at a variety of pressures, for the particular case of very small electric fields at low temperatures.

The only exception to the above picture appears to be in the case of negative ions under pressures greater than about 12×10^5 Pa, when the transition rate remains relatively small and depends much less strongly on the electric field (Zoll & Schwarz 1973). At temperatures near 0.5 K, where the density of the excitation gas becomes small, it is therefore possible to accelerate bare ions up to the Landau critical velocity for roton creation, and to maintain them at this velocity over distances of several millimetres (Rayfield 1966, 1968). Neeper (1968) and Neeper & Meyer (1969) reported, however, that the proportion of bare ions in the current fell rapidly with temperature until, below 0.3 K, the current consisted entirely of charged rings.

The behaviour of charged vortex rings at temperatures below 0.6 K, where they suffer little energy loss, has been investigated in detail by Rayfield & Reif (1964). At higher temperatures vortex rings can only exist in equilibrium if a static electric field is provided in order to replace the energy being lost through the drag of the excitation gas, and a detailed discussion of the influence of vortices on ion motion in this temperature range has been given by Padmore (1972*a*).

Under the influence of an electric field there is a finite probability of the ion escaping from the vortex to which it is bound. Donnelly & Roberts (1969) have developed a stochastic theory of this process, which they treat as the escape of a Brownian particle over the potential barrier formed by the combined vortex and electric potentials. The depth of the vortex potential well is closely related to the volume of the ion, so that the positive ion with its radius of 0.6 nm is less strongly bound to a vortex than a negative ion whose radius is between 1.0–1.6 nm.

In considering the application of these ideas to the motion of ions in a field emission or ionization cell we note that a significant factor will be the very large electric field in the source region. Using the intercepts $V_0 = F_s r_s$ on plots such as those of figure 13, we can estimate the values of F_s. For field ionization, where $V_0 \approx 10^3$ V and r_s is the radius of curvature of the tip itself, which on the basis of earlier work ≈ 100 nm, we conclude that $F_s \approx 10^{10}$ V m^{-1}. This is, of course, the field at the interface between the metal tip and the solid helium which surrounds it; that at the edge of the liquid will therefore be *ca.* 10^9 V m^{-1}. In the case of field emission $V_0 \approx 600$ V but, in view of the gaseous contributions to the generating mechanism, it is by no means clear what value should be taken for r_s; but, even if the effective source radius was 10^2 larger than the radius of curvature of the tip, F_s would still be *ca.* 10^8 V m^{-1}.

Bruschi, Maraviglia & Mazzoldi (1966) have measured the threshold field at which negative ions start to nucleate vortex rings as $4 \times 10^8 \exp(-7.7/T)$ in V m^{-1} at s.v.p. which would imply that, even at temperatures near T_λ, ions will have a large probability of creating vortex rings in the very high electric field immediately after they leave the emitter. They also found that the threshold field for negative ions showed a relatively weak dependence on pressure below 12×10^5 Pa. One may expect that on account of their larger mobility, the threshold field for positive ions will be somewhat smaller.

We conclude, therefore, that in He II virtually all ions form charged vortex rings a very short time after leaving the emitter. The exception to this will, of course, be the case of negative ions at pressures above 12×10^5 Pa.

The extent to which the presence of charged vortices affects the emission characteristics will depend crucially on the magnitude of the escape probability: if, as one would expect at the higher temperatures, the ions escape almost immediately from their rings, the vortices will have little effect; but at lower temperatures where escapes are improbable the relatively much smaller

velocity of charged vortices would tend to increase the spacecharge density and thus have the effect of reducing the emission current. A qualitative explanation of the observed current temperature characteristics can thus be given in terms of the influence of vortices: at high temperatures the escape probability is large, so that the current is proportional to the bare ion mobility according to equation (4), and the current rises with falling temperature; as the temperature is reduced the escape probability P falls until the time spent as a bare ion after escape is comparable with P^{-1}, at which temperature the current will pass through a maximum; and a further reduction of the temperature will cause ions to spend a progressively larger proportion of their transit time trapped on slowly moving vortices, and will therefore result in a decrease in current. The sensitivity to pressure of the temperature at which the maximum in the field emission current occurs can therefore be attributed to changes in P resulting from changes in the radius of the negative ion; and the insensitivity to pressure of the field ionization current maximum can, by a similar argument, be attributed to the insensitivity of the positive ion radius to changes in pressure.

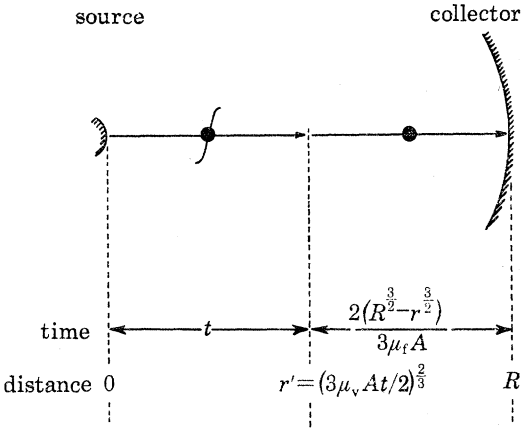

FIGURE 20. Diagram illustrating the model employed in deriving (20). All ions create vortices and are trapped by them immediately they leave the source; but some escape after time t and then proceed as free ions to the collector. Not illustrated are the ions which remain bound to vortices during their whole transit.

Conduction at the lowest temperatures, which is discussed in § 4 (*e*), is not understood in detail, but clearly involves a tangle of charged vorticity rather than individual charged vortex rings. The increase with pressure above 12×10^5 Pa of the field emission current in this temperature range (see figure 9) can be attributed to an increasing proportion of bare ions in the current owing to the decrease with pressure of the vortex nucleation probability: at these temperatures, all bare ions will be travelling at the Landau critical velocity for roton creation ($v_L \approx 50\,\mathrm{m\,s^{-1}}$) and, because v_L is more than two orders of magnitude larger than the average velocity of the vortex borne charge, they will contribute negligibly to the spacecharge density.

(*c*) *The escape probability*

To place the above ideas on a more quantitative basis we consider the passage of N_0 ions across a spherically symmetrical chamber of radius R, in the temperature range where P^{-1} is comparable with their total transit time. It has already been shown that even a model which approximates the electric field in the drift space by a constant average value is able to account quite well for the temperature dependence of the current in this range (McClintock 1973*c*);

but we now consider a rather more realistic model, illustrated in figure 20, in which the electric field is given by equations (3) and (4), as

$$F = Ar^{-\frac{1}{2}}, \tag{8}$$

where

$$A = \tfrac{1}{2}(V_s - V_0)\, R^{-\frac{1}{2}}. \tag{9}$$

We suppose that *all* the ions create vortex rings at the source, which we assume to have a negligibly small radius.

We wish to estimate the average ionic transit time $\bar{\tau}$ across the chamber and then use the fact that, since the spacecharge density remains constant, the resultant current $i \propto \bar{\tau}^{-1}$. The sum of all the transit times $N_0\bar{\tau}$ is made up of three terms: (i) the sum t_1 of all the times spent bound to vortices before escape; (ii) the sum t_2 of all the times spent as free ions, after escaping; and (iii) the sum t_3 of all the times spent bound to vortices by ions which do not escape at all during their transits. The number of ions remaining bound after a time t is $N_0 e^{-Pt}$; in an interval dt, Pdt of them escape; and so the first term is

$$t_1 = \int_0^{t_v} PtN_0 \exp(-Pt)\, \mathrm{d}t, \tag{10}$$

where t_v is the time which a vortex borne ion would take to reach the collector if it did not escape during the transit. The time t taken to reach a radial distance r is $\int_0^r \mathrm{d}r/v$, so that, using $v = \mu F$ together with (8), we find

$$t = 2r^{\frac{3}{2}}/3\mu_v A, \tag{11}$$

which can be inverted to give the distance travelled by a vortex bound ion from the source in time t

$$r = (3\mu_v At/2)^{\frac{2}{3}}, \tag{12}$$

where μ_v is the vortex limited mobility. The time taken to travel as a free ion from r to R is $\int_r^R \mathrm{d}r/v$ which, by similar arguments to those employed in obtaining (11), is just $2(R^{\frac{3}{2}} - r^{\frac{3}{2}})/3\mu_f A$, where we use μ_f to denote the mobility of a free ion. Thus the sum of times taken by the $N_0 P \exp(-Pt)\,\mathrm{d}t$ ions which escape in the interval of time dt, at a time t after leaving the source, to reach the collector after their escapes is

$$\mathrm{d}t_2 = N_0 P \exp(-Pt)\,[2(R^{\frac{3}{2}} - r^{\frac{3}{2}})/3\mu_f A]\,\mathrm{d}t.$$

This expression can be simplified if we note, using (12), that

$$t_v = 2R^{\frac{3}{2}}/3\mu_v A \tag{13}$$

and define

$$t_f = 2R^{\frac{3}{2}}/3\mu_f A, \tag{14}$$

which is the time a free ion would take to travel from source to collector. Inserting (12), (13) and (14) we find that

$$t_2 = \int_0^{t_v} t_f(1 - t/t_v)\, PN_0 \exp(-Pt)\,\mathrm{d}t. \tag{15}$$

The time spent by an ion in crossing the chamber on a vortex is just t_v, and since $N_0 \exp(-Pt_v)$ of the ions are able to do so

$$t_3 = t_v N_0 \exp(-Pt_v). \tag{16}$$

Adding together equations (10), (15) and (16), dividing by N_0, and rearranging slightly, we find

$$\bar{\tau} = Pt_f \int_0^{t_v} \exp(-Pt)\,\mathrm{d}t + P(1 - t_f/t_v) \int_0^{t_v} t \exp(-Pt)\,\mathrm{d}t + t_v \exp(-Pt_v).$$

Making the approximation $(1-t_f/t_v) \approx 1$ since μ_f is greater than μ_v by a factor of about 10^3 in the temperature range of interest, evaluating the integrals, and then rearranging the equation slightly, we obtain a relatively simple relation for the mean transit time

$$\bar{\tau} = (P^{-1} + t_f)\,[1 - \exp(-Pt_v)]. \tag{17}$$

We note that $\bar{\tau} \to t_f$ as $P \to \infty$, and $\bar{\tau} \to t_v$ as $P \to 0$, as required.

Under spacecharge limited conditions

$$i = M\bar{\tau}^{-1}, \tag{18}$$

where M is a constant. We can find M by combining equations (9), (14), (17) and (18) in the limit of large P, yielding

$$i = 3M\mu_f(V_s - V_0)/4R^2, \tag{19}$$

which, through comparison with equation (4), demonstrates that

$$M = 4\alpha\epsilon(V_s - V_0)\,R/3(3.097 \times 10^5)^2.$$

We conclude, therefore, that

$$i = 1.389 \times 10^{-11}\,\alpha\epsilon(V_s - V_0)\,R\{(P^{-1} + t_f)\,[1 - \exp(-Pt_v)]\}^{-1}. \tag{20}$$

This relation can, in principle, be used to determine P from measurements of the field emission and ionization characteristics: α may be found by comparing high temperature values of $i/(V_s - V_0)^2$ with the absolute value of the mobility at the same temperature, measured by another method, as described in §4(*a*); V_0 may be obtained from the intercept of plots such as those of figure 13; t_v and t_f we can obtain from (13) and (14) respectively, deriving the required values of μ_v and μ_f by extrapolating the measurements described in §4(*a*) to higher and lower temperatures respectively.

A difficulty with the latter procedures is that, while there are good theoretical grounds for extrapolating μ_f by fitting to a relation of the form $\mu = B\exp(\Delta/kT)$, where B is a constant and Δ is the roton energy gap, the mechanism underlying the vortex limited mobility is not understood and there is not, therefore, any theoretical justification for using a particular extrapolation equation. To avoid this problem, we have preferred to consider (17) only in the high temperature limit where $\exp(-Pt_v) \ll 1$, so that, to a good approximation,

$$\bar{\tau} = P^{-1} + t_f. \tag{21}$$

The inaccuracies introduced by using (21) rather than (17) are less than 5% provided that $P > 140$ or $270\ \mathrm{s}^{-1}$, for negative or positive ions respectively, with an emitter potential of 3000 V. Combining (9), (14), (18) and (21) we obtain

$$P = 0.75\,(V_s - V_0)\,R^{-2}[(i'/\mu')\,i^{-1} - \mu_f^{-1}]^{-1}, \tag{22}$$

where i' is the current which flows when the mobility is μ' either in He I or in He II within a temperature range where vortices have a negligible effect on the transit time. We have taken for i'/μ' the average of several measurements at temperatures at least 0.3 K above that of the maximum in the current, and for μ_f at 10^5 Pa we have used Schwarz's (1972) s.v.p. data. To obtain values of μ_f for positive ions at higher pressures we have used the relation $\mu_f = B\exp(\Delta/kT)$ in conjunction with the s.v.p. data, and we have assumed that the negative and positive ion mobilities are the same above 12×10^5 Pa (Meyer & Reif 1961). In fact, the values of P obtained turned out to be rather insensitive to the precise value of μ_f used in their derivation except, of course, at temperatures near those of the maxima in the current.

In figure 21 we show as functions of T^{-1} some typical values of P derived from our data using (22). Within experimental error, a relation of the expected (Donnelly & Roberts 1969; Padmore 1972*a*) form, $P = C \exp(-\Delta U/kT)$, where C and ΔU are constants, is followed in most cases. We note that the derived values of P exhibit qualitatively the behaviour expected: the gradients of the graphs have much larger magnitudes for negative than for positive ions, corresponding to larger values of ΔU in the former case; and for negative ions at any particular temperature,

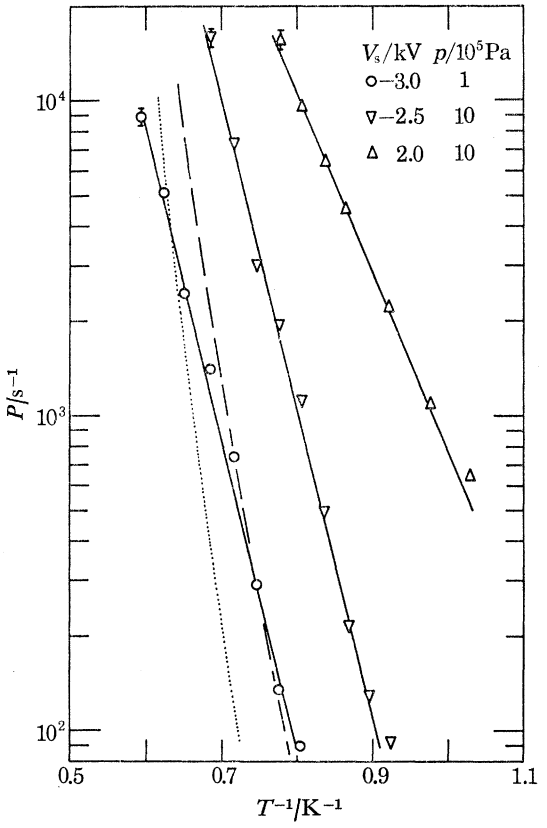

FIGURE 21. Values of the escape probability P of positive and negative ions from vortices as a function of (temperature T)$^{-1}$ for various emitter potentials V_s and pressure p, derived by using (22). The straight lines, which have been drawn by eye through the data points, correspond to the equations: $P = 1.26 \times 10^{19} \exp(-23.5/T)$ for negative ions with $V_s = 3000$ V at $p = 10^5$ Pa; $P = 4.06 \times 10^{19} \exp(-21.9/T)$ for negative ions with $V_s = 2500$ V at $p = 10 \times 10^5$ Pa; and $P = 3.22 \times 10^8 \exp(-12.9/T)$ for positive ions with $V_s = 3000$ at $p = 10 \times 10^5$ Pa; and the bars on the points refer to random noise in the current measurements. The dotted and dashed curves refer to values of P calculated from the Donnelly & Roberts (1969) theory for negative ions at $p = 10^5$ Pa, and either $F = 6 \times 10^5$ or 7×10^5 V m^{-1} respectively.

P increases rapidly with pressure, owing to shrinkage of the electron bubble and a corresponding reduction in ΔU. These values of P must, of course, refer to some average electric field in the cell, so that comparison with other measurements is unfortunately not straightforward. The criterion suggested earlier by McClintock (1973*c*), that the relevant electric field F' might be that at the average radius of escape when half the transit time is spent trapped on a vortex and half as a free ion, is unsatisfactory in that it is not easily applicable: although it is straightforward to show that $F' = (V_s - V_0)(\mu_f/\mu_v)^{\frac{1}{3}}/2R$, we are ignorant of the value and possible temperature dependence of μ_v within the range of interest.

A proper comparison of our experimental data with the Donnelly & Roberts escape theory would, of course, require that we replace the above approximate analysis leading to (20) with a more sophisticated calculation in which explicit account was taken of the dependence of P upon F. We do not, however, feel that this procedure would be justified while still retaining the approximate form (8) for F and, since a solution of the Poisson equation (1) from first principles for a mixture of free ions and charged vortices constitutes a formidably difficult problem, we have not attempted to develop a more exact analysis. We can, however, demonstrate that the values of P derived from the data on the basis of our simple model are at least of the right order of magnitude. The dotted and dashed curves of figure 21 refer to values of P at 10^5 Pa calculated from the Donnelly & Roberts theory for electric fields respectively of 6×10^5 and 7×10^5 V m^{-1} corresponding, for $V_s = 3000$ V, to positions 1.0 and 0.7 mm from the emitter.

An alternative and somewhat more empirical method of testing our model is to investigate the way in which the temperature T_{max} of the maximum in the current varies with pressure and emitter potential: we can arbitrarily choose a value of F' such that the model yields the correct value of T_{max} at one particular value of p or V_s, and then see how the predicted dependence of T_{max} on p or V_s compares with experiment. To find the T_{max} predicted by the model, we have maximized (20) with respect to temperature. In doing so we have assumed that within the temperature range of interest we may write $P = C\exp(-\Delta U/kT)$ and $\mu_t = D\exp(\Delta/kT)$ where C, D, ΔU and Δ are constants, and have ignored $\exp(-Pt_v)$ in comparison to unity. Under these conditions

$$T_{max} = (\Delta U + \Delta)/k \ln[4CR^2\Delta/3\Delta UD(V_s - V_0)]. \tag{23}$$

In figure 22*a* we show a comparison between our experimental values of $T_{max}(p)$ and the behaviour predicted by (23), for both positive and negative ions; and in figure 22*b* we show a similar comparison for the case of $T_{max}(V_s)$. In computing the theoretical curves: we have calculated ΔU and C from the Donnelly & Roberts (1969) escape theory using the negative ion radii deduced by Springett & Donnelly (1966) and the positive ion radius, assumed independent of pressure, deduced by Parks & Donnelly (1966); we have assumed that, with $V_s = 2000$ V, $F' = 5 \times 10^5$ V m^{-1}; we have obtained Δ and C at low pressure from Schwarz's (1972) mobility data; we have extrapolated values of Δ for positive ions at higher pressures by assuming that $\mu(p) = \mu(0)\exp[\Delta_r(p) - \Delta_r(0)]$, where Δ_r is the roton energy gap (Meyer & Reif 1961); and we have assumed that the negative ion mobility is pressure independent below 10×10^5 Pa, but that, at higher pressures, it scales with the positive ion mobility as observed by Meyer & Reif.

It is immediately obvious that the value of F', which was chosen to fit the negative ion data at low pressure, results for positive ions in severe disagreement between experimental values of T_{max} and those predicted by (23). This disagreement cannot be resolved by choosing a different value of F' because, in order that T_{max} in (23) should take its experimentally observed value, it would be necessary to assume that F' was considerably smaller than the field at $r = R$, which is its minimum value in the cell. We conclude, therefore, that our simple model is unable quantitatively to account for the positive ion $i(T)$ characteristics. The reason is probably connected with multiple escape–trapping–escape processes, as we discuss in more detail below. In the case of negative ions, however, the model seems able to account quite satisfactorily for the $T_{max}(p)$ and $T_{max}(V_s)$ characteristics provided, of course, that we make the plausible assumption

$$F' = 5 \times 10^5 \text{ V m}^{-1} \quad \text{for} \quad V_s = 2000 \text{ V}.$$

It is interesting to note a very simple physical reason for the, at first sight, remarkable insensitivity of T_{max} to changes in V_s: at any given temperature, an increase in V_s acts directly on ΔU in the exponent of the expression for P and therefore greatly increases the escape probability, which would then tend, therefore, to bring about a substantial decrease of T_{max}. However, in this temperature range, a decrease of T results in a significant increase of ρ_s, which appears as a factor in the expression for ΔU (Donnelly & Roberts 1969), thus tending to *increase* ΔU and hence T_{max}. It is thus the temperature dependence of ρ_s which is responsible for very largely counteracting the influence on T_{max} of changes in V_s or R.

The observed dependence of T_{max} on both V_s and p is, however, even less than predicted by the model, and the reason for this situation remains obscure. We observe, however, that quantitative agreement between the Donnelly & Roberts theory and direct measurements of P is not entirely satisfactory (see, for example, figure 9*b* of Donnelly & Roberts 1969) possibly owing to reasons which have been discussed by Padmore (1972*b*). In addition, our model has introduced a number of approximations, the most important of which is that the electric field profile in the cell is always that given by equations (8) and (9), even when vortices are present. It is evident that in reality the trapping/escape process *will* perturb the field so that, to this extent, our analysis must be regarded only as a first approximation.

In order to illustrate the interplay of the various physical phenomena which give rise to the observed $i(T)$ characteristics we show in figure 23, as functions of temperature, some of the characteristic times involved in our model. $\bar{\tau}$, t_v, t_f and P^{-1} have been determined by fitting equations (13), (14), (17) and (20) to our experimental data at $p = 10^5$ Pa, $V_s = 3000$ V. Also indicated on the diagram are the transit time t_L for an ion travelling at the Landau velocity, and P_a^{-1}, where P_a is the probability of an ion escaping through annihilation of the element of vortex on which it is trapped. P_a has been estimated by taking Sitton & Moss's (1972) relation for Vinen's F_2 parameter, and assuming that all the energy extracted by the ions from the electric field goes into the creation of vortex lines. There is, however, reason to impugn the validity of using the Sitton & Moss relation below 0.5 K (see § 4 (*e*)); and the latter assumption is certainly inappropriate above about 0.6 K owing to the rapidly increasing effect of normal fluid drag on a charged vortex. For these reasons, our calculated values of P_a^{-1} are probably too large below 0.5 K and too small above 0.6 K: the curve shown in figure 23 should therefore be treated with considerable caution.

In reality, P_a is likely to *decrease* as T increases above 0.6 K because the drag arising from the increased roton density will reduce the vortex creation rate $\dot{L}_c$; and, since P_a must be negligible above T_{max} where the ionic trapping time is very small, it is clear that the curves for P_a^{-1} and P^{-1} must cross somewhere between these temperatures. Because the presence in the chamber of a significant proportion of bare ions, which the data and our model suggest is the case above 1.1 K, will itself cause a drastic decrease in $\dot{L}_c$, it seems unlikely that the annihilation escape mechanism will be significant within the temperature range where we have derived values of the escape probability. We conclude, therefore, that the derived values (figure 21) refer to thermally activated escapes; and note that this conclusion appears to be supported by the fact that the observed temperature dependence is similar to that predicted by the Donnelly & Roberts theory.

Our model takes no explicit account of the possibility of repeated escape–trapping–escape. processes. These will, however, certainly be occurring for $r < r_c$, where r_c is the radius at which the electric field in the cell takes the critical value F_c for nucleation of vortex rings. Provided $r_c \ll R$ the emitter can still be treated as a point source of charged vorticity, and the model will be applicable; but as the temperature is reduced a situation will eventually arise where this inequality is

no longer obeyed and the model, in its simple form, will no longer be appropriate. Using Bruschi, Maraviglia & Mazzoldi's (1966) values of F_c for negative ions, we find that $r_c = \frac{1}{10}R$ at about 1.3 K for negative ions; for positive ions the critical radius will probably, owing to their greater mobility, be reached at a slightly higher temperature. It is clear, therefore, that the values of P for negative ions in figure 21 should be unaffected by repeated escape–trapping–escape processes; and additional support for this conclusion can be gained from the non-uniformity of the electric field and the relatively small values of P, which together imply that an escape takes place in a very much smaller electric field than that in which the preceding nucleation event occurred, thus rendering another nucleation less probable.

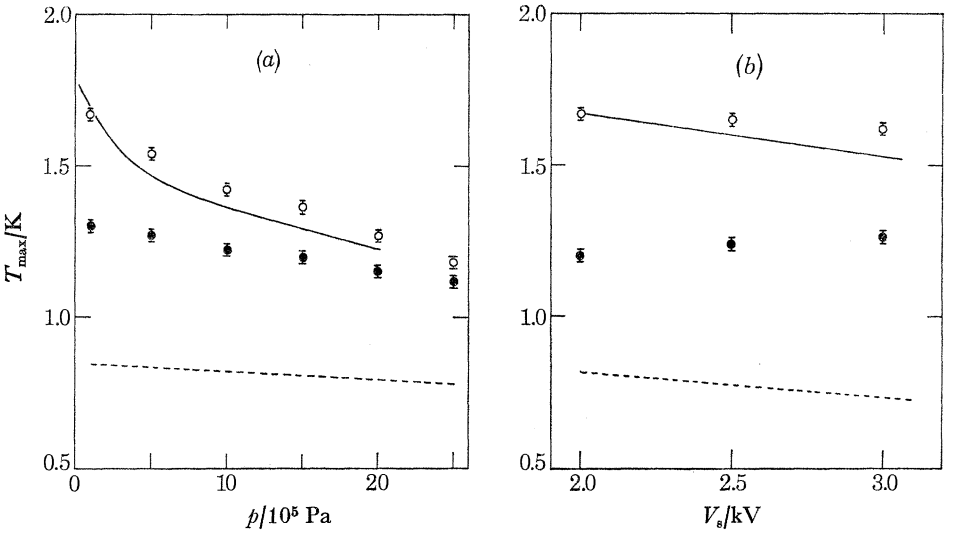

FIGURE 22. Temperatures T_{max} of the maxima in the field emission and field ionization currents: (*a*) plotted against pressure p for a constant average electric field of $F' = 5 \times 10^5$ V m^{-1}, and (*b*) plotted against V_s for a pressure of $p = 10^5$ Pa (negative ions) and $p = 10 \times 10^5$ Pa (positive ions). The experimental values (points: open circles, negative ions; filled circles, positive ions) are compared with those calculated using equation 23 (full curves), assuming in each case that $V_s = 2$ kV corresponds to $F' = 5 \times 10^5$ V m^{-1}.

The values of P derived for positive ions from the model (figure 21) are all for $T < 1.3$ K, where our single-escape model is not strictly applicable. It is not entirely surprising, therefore, that our values are about two orders of magnitude lower than those which may be extrapolated from Cade's (1965) measurements near 0.5 K on the basis of the Donnelly & Roberts (1969) theory. We note that Padmore (1972*a*) has reported these extrapolated values to be consistent with Bruschi, Mazzoldi & Santini's (1968) measurements of positive ion drift velocities in large electric fields above 1.0 K, which adds weight to our conclusion that the values of P for positive ions in figure 22 are too low. A proper treatment of our data would require that explicit account was taken of repeated escape–trapping–escape events, as has been accomplished by Padmore (1972*a*) in his calculations of drift velocities in high uniform fields above 1 K. To employ this type of treatment in the case of a nonuniform electric field would be difficult and, in view of all the uncertainties, we have not felt it justified to attempt development of a more sophisticated model.

We note that, below 1 K, equation (20) again becomes applicable because the probability of thermally activated escape is negligible, and conduction occurs through the vortex limited mechanism discussed in § 4 (*e*).

It is concluded that for both positive and negative ions the model is successful in accounting qualitatively for the observed $i(T)$ emission characteristics in terms of the existing understanding of He II; that quantitative agreement between experiment and theory is satisfactory in the case of field emission; and that the quantitative disagreement in the case of field ionization can be understood in terms of multiple escape–trapping–escape events.

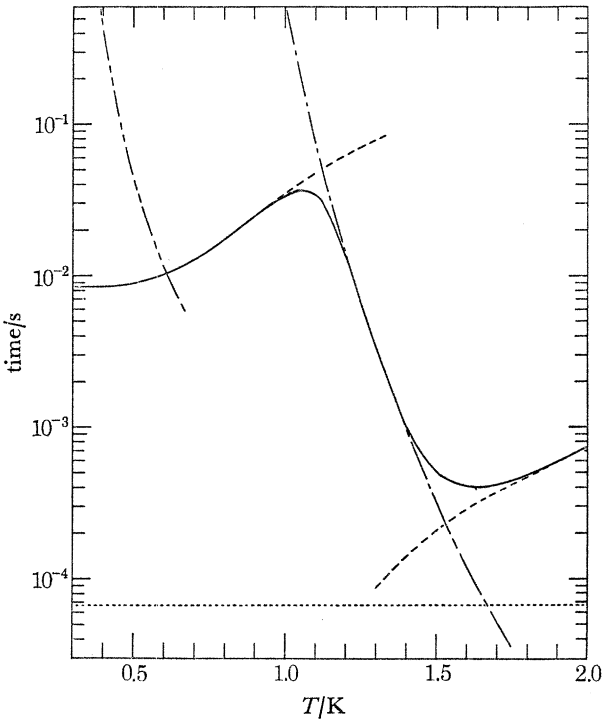

FIGURE 23. Some characteristic times in the model developed to account for the temperature dependence of the emission currents, plotted as functions of temperature. The full curve represents $\bar{\tau}$ from equation 17 fitted to a set of experimental data at $V_s = 3000$ V, $p = 10^5$ Pa. The agreement is extremely close except in $0.9 < T < 1.2$ K where, because of *multiple* creation–trapping–escape events, the model is not expected to be applicable in detail. In the fitting procedure t_v and t_i (upper and lower small-dashed curves, respectively) have been calculated using (9), (13) and (14) assuming Schwarz's (1972) values of μ_i; extrapolating the relation $\mu_v = \mu_{v0}[1+230 \exp(-4.3/T)]$, which fits the data accurately below 0.8 K, to higher temperatures; and values of M in (18) and of μ_{v0} have been selected so as to give quantitative agreement with the experimental data in the limits of high and low temperatures respectively. The expression

$$P = 1.3 \times 10^{10} \exp(-23/T)$$

has been chosen to give agreement with the data in the range $1.2 < T < 1.6$ K, and the equation has then been extrapolated to higher and lower temperatures (dash–dot curve). Also included in the diagram are t_L (dotted curve), the time an ion would take to cross the chamber at the Landau velocity; and P_a^{-1} (dash–double-dot curve), the average trapping period prior to escape through vortex annihilation which has been calculated on the basis of assumptions which are discussed in the text. It should be noted that the latter curve is expected to rise steeply again at higher temperatures, crossing the P^{-1} curve near 1 K.

(*d*) *The nucleation probability*

We now consider the particular case of negative ions at pressures above 12×10^5 Pa, and we suppose the temperature to be in the range below 0.8 K where the probability of thermally activated escapes is negligible. This is the opposite extreme situation to that analysed in §4(*c*): now all the charge carriers start as bare ions from the source and have a finite, but not necessarily large, probability of nucleating vortex rings during their transit to the collector. Takken (1970) has

discussed the creation of rotons by an ion moving near v_L on the basis of a wave radiation model, and has concluded that the process sets in with such rapidity at $v = v_L$ that it should be exceedingly difficult experimentally to cause ions to exceed this velocity. He estimates that, even for an electric field of $10^7\,\mathrm{V\,m^{-1}}$, $(v - v_L)/v_L \approx 1\%$. This prediction has not been tested experimentally but, in setting up a model to describe the field emission measurements, we shall make the simplifying assumption that all bare ions in our cell move at the same velocity, v_L. As we have already reported (Phillips & McClintock 1974), it is possible to proceed in a manner very similar to that described in §4(*c*) for deriving values of P, and thus to deduce values of the nucleation probability ν.

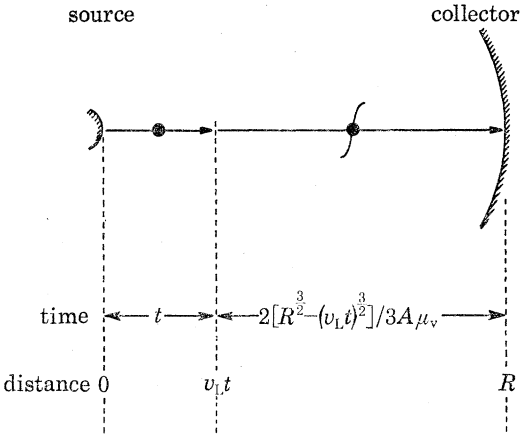

FIGURE 24. Diagram illustrating the model employed in deriving (32). Charge leaves the source in the form of free ions; but after a time t some of these create vortices and are trapped by them; and they remain trapped during the remainder of their transit to the collector. Not illustrated are the ions which reach the collector without nucleating vortices or being trapped.

We assume that the electric field distribution is that given by equations (8) and (9), and suppose that it is not greatly perturbed by the complementation of the vortex borne current by a proportion of fast moving bare ions. Considering the model illustrated in figure 24, we compute the average transit time $\bar{\tau}$ of N_0 ions from source to collector. The sum of all the transit times $N_0\,\bar{\tau}$ is made up of three terms: (i) the sum t_1 of all the times spent as bare ions prior to nucleation and trapping; (ii) the sum t_2 of all the subsequent times spent bound to vortices; (iii) the sum t_3 of all the times in transit of those ions which fail altogether to nucleate rings. The number of bare ions remaining after time t is $N_0 \exp(-\nu t)$; in an increment of time $\mathrm{d}t$, $\nu\,\mathrm{d}t$ of them nucleate vortex rings; and so the first term is

$$t_1 = \int_0^{t_f} \nu t N_0 \exp(-\nu t)\,\mathrm{d}t, \tag{24}$$

where t_f is the time taken to cross the chamber as a bare ion. The additional time taken for an ion captured after time t to reach the collector is $\int_{v_L}^{R} \frac{\mathrm{d}r}{v}$ which, remembering $v = \mu F$ and by using equation (8), becomes

$$2[R^{\frac{3}{2}} - (v_L t)^{\frac{3}{2}}]/3A\mu_v.$$

Thus
$$t_2 = \int_0^{t_f} (2/3A\mu_v)\,[R^{\frac{3}{2}} - (v_L t)^{\frac{3}{2}}]\,N_0\,\nu \exp(-\nu t)\,\mathrm{d}t.$$

Noting that
$$t_f = R/v_L, \tag{25}$$

and that t_v as given by (13) is still the transit time for a wholly vortex borne ion, we obtain

$$t_2 = \int_0^{t_f} t_v[1-(t/t_f)^{\frac{3}{2}}]\, N_0 \nu \exp(-\nu t)\, \mathrm{d}t. \tag{26}$$

Since $N_0 \exp(-\nu t_f)$ of the ions reach the collector without nucleating rings,

$$t_3 = t_f N_0 \exp(-\nu t_f). \tag{27}$$

Adding together (24), (26) and (27), dividing by N_0, we find

$$\bar{\tau} = \int_0^{t_f} \nu t \exp(-\nu t)\, \mathrm{d}t + \int_0^{t_f} t_v[1-(t/t_f)^{\frac{3}{2}}]\, \nu \exp(-\nu t)\, \mathrm{d}t + t_f \exp(-\nu t_f).$$

Evaluating the simple integrals, and rearranging slightly,

$$\bar{\tau} = (t_v + \nu^{-1})\,(1-\exp(-\nu t_f)) - [t_v/(\nu t_f)^{\frac{3}{2}}]\, I(\nu t_f), \tag{28}$$

where

$$I(\nu t_f) = \int_0^{\nu t_f} (\nu t)^{\frac{3}{2}} \exp(-\nu t)\, \mathrm{d}(\nu t). \tag{29}$$

Since the incomplete gamma function, of which tabulated values are available (Abramowitz & Stegun (1965)), is defined as

$$\gamma(a, x) = \int_0^x y^{a-1} \exp(-y)\, \mathrm{d}y,$$

we see that

$$I(\nu t_f) \equiv \gamma(\tfrac{5}{2}, \nu t_f). \tag{30}$$

Neglecting ν^{-1} in comparison with t_v in the first parentheses of (28), and combining (28), (29) and (30), we obtain

$$\bar{\tau} = t_v[1-\exp(-x) - \gamma(\tfrac{5}{2}, x)/x^{\frac{3}{2}}], \tag{31}$$

where we have set $\nu t_f = x$. We can obtain the current from the average transit time by the same method as was used in deriving (20). We find

$$i = 1.389 \times 10^{-11}\, \alpha\epsilon (V_s - V_0)\, R\{t_v[1-\exp(-x) - \gamma(\tfrac{5}{2}, x)/x^{\frac{3}{2}}]\}^{-1}. \tag{32}$$

This relation can, in principle, be used to derive values of x and hence ν from measured values of the current; but we have, in practice, found it convenient to measure the ratio $\phi = i/i_0$, where i_0 is the current which would flow if $x \gg 1$ and no bare ions were present, and then to compare our data with

$$\phi = [1-\exp(-x) - \gamma(\tfrac{5}{2}, x)/x^{\frac{3}{2}}]^{-1}. \tag{33}$$

To obtain values of i_0 we have extrapolated linearly the weak negative dependence of the current on pressure below 12×10^5 Pa (see, for example, the characteristics below 0.8 K in figure 9) to higher pressures. We have obtained values of ν from our experimental data graphically, by using plots of ϕ such as graph II of figure 25 to find the value of x corresponding to our measured value of ϕ. For R we have taken its average value of 4 mm. Typical results of this procedure are shown in figure 26*a*, where the bars on the points refer to experimental errors in measuring the currents. In deriving the temperature dependence of ν (figure 26*b*), rather than using the extrapolation procedure, we have taken for i_0 the current at 10×10^5 Pa for each temperature, which may introduce an additional error of about $+2\,\%$ in ν.

It is difficult to assess quantitatively the reliability of values of ν deduced in this way. As in the calculation of P, the largest single source of systematic error is probably our implicit assumption

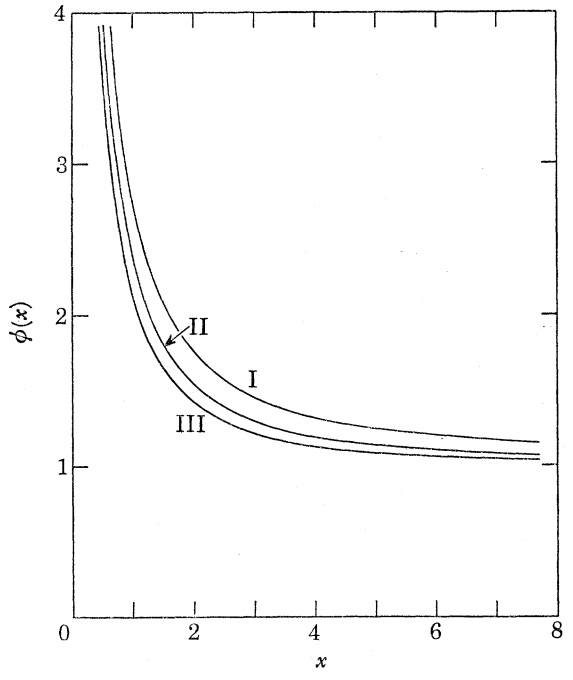

FIGURE 25. Theoretical plots of $\phi = i/i_0$, where i is the total current and i_0 is the vortex borne component, as functions of $x = \nu t_t$, where ν is the vortex nucleation probability and t_t is the time taken by a free ion in crossing from emitter to collector. Curve I represents the equation $\phi = x[\exp(-x) - 1 + x]^{-1}$, which was derived on the assumption of a uniform electric field in the chamber; curve II represents (33) which, as discussed in the text, was derived on the assumption that the field $F \propto r^{-\frac{1}{2}}$; and curve III represents the equation $\phi = x[2\{\exp(-x) - 1\}\{1 + x^{-1}\} + x + 2]^{-1}$, which was derived on the assumption that $F \propto r^{-1}$. Curve II has been used in deriving the values of ν shown in figure 26.

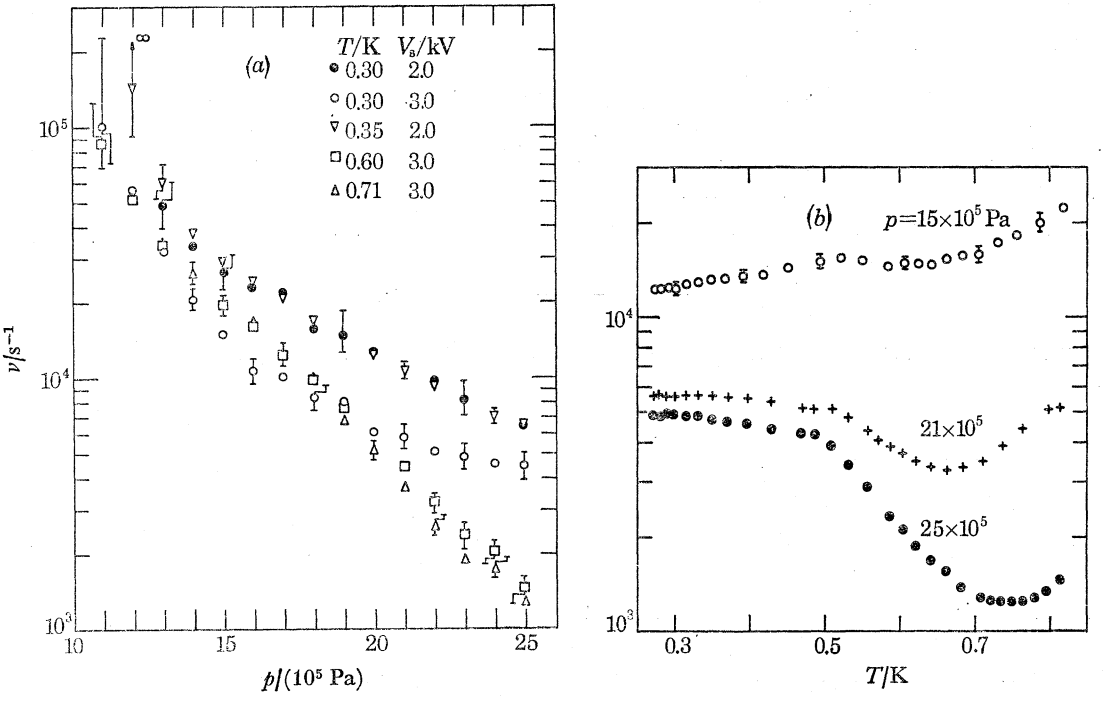

FIGURE 26. The nucleation probability ν of vortices by negative ions, derived by using equation (33) in conjunction with the experimental data: (*a*) as a function of pressure p for various temperatures T and emitter potentials V; and (*b*) as a function of temperature for three values of p.

that the radial electric field profile is unaffected by the introduction of bare ions. In fact, as the pressure is increased, not only does the proportion of bare ions increase, but there will also tend to be a decrease in the density of vortex bound ions close to the emitter together with a balancing increase in vortex bound charge near the collector. The resulting alteration in the field profile will act in the direction of increasing the current; close to the emitter most of the current is carried by bare ions which travel at velocity v_L, independent of electric field; but near the collector, where many of these ions have been captured by vortices, an increase in electric field will result in a corresponding increase in their drift velocity. A simple calculation, solving the Poisson equation for the electric field on the assumption of a constant vortex limited mobility and using our derived values of ν as the first approximation, suggests that at 20×10^5 Pa ν in figure 26 may be 10 % too low for this reason.

The effect of deviations from our assumed $F \propto r^{-\frac{1}{2}}$ field profile for purely vortex limited conduction can be considered by reference to figure 25. If the profile were instead $F \propto r^{-1}$ (corresponding to curve III), which would be the consequence of conduction *only* by bare ions all moving at the same drift velocity, independent of electric field, then our derived values of ν would be too large by about 25 %; but because, in reality, the current is never more than a small fraction of that which would occur under the controlling influence of a spacecharge of ions all moving at v_L, we feel that the profile will be much closer to the $r^{-\frac{1}{2}}$ law which we assumed in deriving (33).

The consequences of our having ignored the possibility of ion escapes through vortex annihilation are harder to assess. As shown in figure 23, the annihilation escape rate may become increasingly important below 0.6 K (but see the discussion in the next subsection, which suggests that the calculated value of P_a^{-1} in figure 23 may be substantial overestimates). Any escape mechanism might have the effect of causing values of ν derived using (33) to be smaller than in reality. We note, however, that there seems to be no reason why the escape rate should change as the pressure is altered at constant temperature: although the total current increases with pressure, the density of the vortex borne charge, which takes energy from the electric field and converts some of it into new vortex line, does not change. We may therefore hope that any effect of annihilation escapes will have largely or wholly cancelled when we took the ratio ϕ in analysing the experimental data.

No other measurements of ν, with which we might compare our results, have been reported for this particular range of pressures and electric fields. Zoll & Schwarz (1973) have published values of ν measured under pressure in electric fields of up to 2500 V m^{-1} which are, as pointed out previously (Phillips & McClintock 1974), about an order of magnitude smaller than in the present work. Our electric fields are, however, about two orders of magnitude larger than theirs, and so it is quite possible that the two sets of measurements are consistent with each other.

(*e*) *The conduction mechanism below* 0.7 K

In the preceding analyses we have assumed that the drift velocity of the charge carriers at very low temperatures is limited by their being trapped on vortices but, apart from pointing out that our data suggest that an effective mobility can be defined, we have not yet discussed what may be the mechanism responsible for electrical conduction under these conditions. Although we have not succeeded in developing a detailed theory capable of describing the situation, we now discuss briefly some of the physical processes which may be involved. We consider conduction below 0.5 K at low pressure, so that all ions nucleate vortex rings immediately they enter the liquid and the probability of thermally activated escapes will be negligible.

A simple calculation suggests that the presence of individual charged vortex rings is improbable

PHILOSOPHICAL TRANSACTIONS OF THE ROYAL SOCIETY A MATHEMATICAL, PHYSICAL & ENGINEERING SCIENCES

By using (2), (8) and (9) in conjunction with our experimental data it is possible to compute the charge density and we find for example that at $r = \frac{1}{2}R$ for our chamber with $V_s = -3000\,\mathrm{V}$, $P = 10^5\,\mathrm{Pa}$, there will be about 7×10^6 electrons mm^{-3}: their average separation will thus be $5 \times 10^{-3}\,\mathrm{mm}$. If each electron were trapped on an individual charged vortex ring, the rings at this position in the chamber would have energies of about 2000 eV, and corresponding radii of about $4 \times 10^{-2}\,\mathrm{mm}$. Since the average spacing of the rings would be smaller than their diameters by a factor of about 16, the system would clearly be unstable and the rings would become tangled with each other. This result is supported by the failure of our attempts experimentally to observe the charge carriers crossing a field free region, which is a well known characteristic of charged vortex rings. We also note that if the charge in a field emission cell was carried by individual rings then, because their velocity is inversely proportional to their energy, an *increase* of V_s should tend to produce an increase in spacecharge density, and hence a *decrease* in emission current, quite contrary to the experimental observations.

We conclude, therefore, that the conduction mechanism involves the motion of charge through a tangled mass of vorticity. It seems probable that this is similar in nature to thermally generated vorticity at higher temperatures, which has been investigated in great detail by Vinen (1957, 1958). Although the *escape* of charge from thermally generated vorticity for $1.3 < T < 2\,\mathrm{K}$ has been discussed by Sitton & Moss (1972), conduction of charge *through* vorticity does not seem previously to have been described for any temperature range. At the low temperatures we are considering escape of an ion, by any process, would be followed immediately by its creation of, and trapping by, another vortex ring which would grow rapidly until it tangled with its neighbours: it is therefore exceedingly improbable that a significant proportion of free ions will ever be present in the chamber provided, of course, $p < 10 \times 10^5\,\mathrm{Pa}$.

We have considered a number of possible conduction processes, and in particular the following:

(i) motion of ions *along* vortex lines under influence of the electric field, assuming that periodic rejoining of vortex cores at crossing points would provide a mechanism by which the ions could continue towards the collector;

(ii) bodily motion of the whole mass of charged velocity towards the collector;

(iii) a hopping process whereby ions are periodically liberated through vortex annihilation, recreating vortex rings which initially move rapidly towards the collector but which soon become so large that they tangle with the vorticity.

It seems probable that, whatever mechanism is operative in practice, the net ionic drift velocity will depend on the vortex line density.

We can attempt to estimate the vortex line density by assuming: that all the energy acquired by the ions from the electric field goes into creating vortex line; and that annihilation of the lines occurs by the same processes as those which Vinen (1958) has established as being operative above 1 K in thermally generated vorticity. According to Vinen's theory, the destruction of vortex line comes about when two elements of line with opposite circulation approach close enough to annihilate with each other, and the rate $\dot{L}_a$ at which this occurs is

$$\dot{L}_a = F_2 L^2, \tag{34}$$

where F_2 is a temperature dependent constant and L is the length of vortex line per unit volume. For equilibrium the creation rate $\dot{L}_c$ must be equal to $\dot{L}_a$. Considering the chamber as a whole, and not taking account of local equilibrium at different radii,

$$\dot{L}_c = iV_s/E', \tag{35}$$

where the energy per unit length of vortex line,

$$E' = (\rho_s h^2/4\pi m^2) \ln (b/a_0), \tag{36}$$

where ρ_s is the superfluid density, m the mass of a ^{4}He atom, a_0 is the vortex core radius, and b the outer radius of the circulating fluid. Using (34) and (35) to equate $\dot{L}_c$ and $\dot{L}_a$ we find the equilibrium vortex line density per square millimetre

$$L_0 = (iV_s/F_2 E')^{\frac{1}{2}}. \tag{37}$$

Inserting Sitton & Moss's (1972) experimental value of $F_2 = 210 \exp(-8.65/T)\,\mathrm{mm^2\,s^{-1}}$, assuming that $b \approx 10^{-5}$ mm, and taking standard values for the other constants we find that for our typical situation of $V_s = 3000\,\mathrm{V}$, $i = 3.5 \times 10^{-8}\,\mathrm{A}$, equation (37) implies $L_0 \simeq 10^{10}\,\mathrm{mm^{-2}}$ at 0.3 K. We note that the rapid temperature dependence of L_0 calculated in this way appears to be inconsistent with our experimental observation that the current at fixed emitter potential is almost independent of temperature below 0.4 K.

The temperature dependence of L_0 and its large calculated value arise from our assumption that F_2 has the same exponential temperature dependence at the lowest temperatures as it has above 1 K: and there is reason to suppose that this may not in fact be the case. The experimental observation that F_2 scales with the roton density N_r above 1 K has led Sitton & Moss (1972) to propose a possible mechanism which may be responsible for the annihilation process. They suggest that two elements of line with opposite circulation, which would tend to move through the liquid parallel to each other under the influence of their mutual flow fields, are driven together by the Magnus force arising from the drag imposed by the normal fluid component. If their suggestion is correct then, owing to the increased relative importance at lower temperatures of the drag arising from interactions with phonons and ^{3}He isotopic impurities, we would not expect F_2 to be proportional to N_r below about 0.5 K. These additional drag mechanisms each vary much more slowly with temperature than that arising from rotons, which may help to explain the apparent temperature independence of our emission currents below 0.4 K.

To obtain a more realistic estimate of the vortex line density at the lower temperatures we use the experimental observation of Rayfield & Reif (1964) that for a vortex ring the attenuation coefficient arising from interactions with phonons, rotons and ^{3}He impurities near 0.4 K has approximately the same value as that arising only from rotons at 0.5 K. Thus, we may approximate F_2 at our lowest temperatures by its roton limited value $210 \exp(-8.65/0.5)\ \mathrm{mm^2\,s^{-1}}$ at 0.5 K. On the basis of this assumption we find that $L_0 \approx 5 \times 10^7\,\mathrm{mm^{-2}}$.

For mechanism (i) above it is not, of course, reasonable to assume that *all* of the energy acquired from the electric field goes into creating vortex line. Motion along a line which has a component down the potential gradient will result principally in heating of the line, and not in stretching of it. Thus (35) will not be applicable, and our calculated values of L_0 must be substantial overestimates. It is not, unfortunately, clear how to calculate the L_0 relevant to (i), nor even how to estimate the ionic drift velocity if L_0 were known, so we have not been able to investigate whether this mechanism could account for the observed transit times.

Mechanism (ii) seems implausible because of the very low linear ion density of about $0.1\,\mathrm{mm^{-1}}$, even assuming the lower of our estimates of L_0. The hydrodynamic forces on any element of vortex line must by a large factor outweigh the forces due to electric field acting on the trapped charge, and so there is no reason to suppose that the vorticity could be moved bodily by the electric field at the estimated ionic drift velocity of about $200\,\mathrm{mm\,s^{-1}}$; and in any event, we would be left with the problem of explaining what happens to the vorticity when it reaches the collector. On very

general grounds, one can argue that hydrodynamic forces will tend to produce an approximately uniform equilibrium distribution of vortex line throughout the chamber, in order to equalize the local energy densities in different regions. Because the creation rate will be largest near the emitter where the electric field is largest we may, in fact, expect a slight net radial outflow of vorticity towards the collector, but it is hard to believe that a purely hydrodynamic effect of this sort could be responsible for the magnitudes of ionic drift velocity which we observe.

We thus are left with (iii), which suggests a possible mechanism by which an ion could negotiate its way through a uniform mass of vorticity. There can be no doubt that vortex annihilation must be occurring in the liquid since otherwise, with a steady creation rate, the line density would soon approach infinity. One is forced to conclude, therefore, that the charges trapped on any element of line must be liberated in the form of free ions when it is annihilated. At these low temperatures a free ion will almost instantly create a charged vortex ring which will move towards the collector, expanding and slowing down as it acquires energy from the electric field. When its diameter becomes comparable with the average spacing of the lines in the vorticity, tangling will occur and the initial situation will be reproduced once more. The ion will thus proceed in a series of short hops whose frequency and length will be determined by the value of L_0. Taking our lower estimate of $L_0 \approx 5 \times 10^7\,\mathrm{mm^{-2}}$ we conclude that the maximum possible radius for an individual vortex ring would be $L_0^{-\frac{1}{2}}/2 = 7 \times 10^{-5}\,\mathrm{mm}$. A ring of this final radius would have a characteristic velocity of about $1\,\mathrm{m\,s^{-1}}$, and its time-averaged velocity between creation and tangling would of course be considerably larger. The net ionic drift velocity which we observe is *ca.* $200\,\mathrm{mm\,s^{-1}}$ so we conclude that, if (iii) is the relevant mechanism, the fraction of the ionic transit time spent as charged vortex rings is very much less than that spent trapped on vorticity awaiting the next escape. The net velocity through this mechanism will, to a good approximation, be $P_a l_v$ where P_a is the escape rate arising from vortex annihilation and l_v is the average distance travelled by rings.

We can estimate l_v by setting

$$\pi L_0^{-\frac{1}{2}} E' = eFl_v,$$

so that

$$l_v = \pi L_0^{-\frac{1}{2}} E'/eF. \tag{38}$$

The annihilation escape probability is given by

$$P_a = \dot{L}_a/L_0, \tag{39}$$

so that the net ionic velocity should be

$$\bar{v} = \pi L_a E'/eFL_0^{\frac{3}{2}}.$$

Since, in equilibrium $\dot{L}_a = F_2 L_0^2$ from (34), we obtain finally

$$\bar{v} = \pi F_2 L_0^{\frac{1}{2}} E'/eF. \tag{40}$$

Inserting our typical mean electric field of $400\,\mathrm{V\,mm^{-1}}$ and assuming again that $L_0 = 5 \times 10^7\,\mathrm{mm^{-2}}$ we find $\bar{v} \approx 2\,\mathrm{mm\,s^{-1}}$, which is smaller than the observed drift velocity by two orders of magnitude. We also note that, assuming $F \propto V_s$ and that L_0 is given by (37), (40) implies that $\bar{v} \propto V_s^{-\frac{1}{4}}$, which is entirely contrary to the experimental results: if an *inverse* power law were really followed then the current would fall with increasing emitter potential. It appears therefore that, although the calculated magnitude of $\bar{v}$ may be wrong merely because of an inappropriate choice of F_2 and hence of L_0, the functional form of (40) suggests that (iii) is not the principal mechanism by which charge is transported through the liquid.

We conclude that the principal conduction mechanism is not (iii) and is unlikely to be (ii);

but may be either (i) or, alternatively, some completely different process which we have not considered here. It seems unlikely that much more progress can be made in reaching an understanding of the situation without further experimental data and, in particular, an independent estimate of L_0 based on another type of measurement. This might perhaps be achieved through thermal conductivity measurements of the type described by McClintock (1970), or through an investigation of second sound attenuation (Bruschi *et al.* 1966). Unfortunately, both these techniques would fail to yield information about L_0 at the lowest temperatures: thermal conduction by phonons is almost unaffected by vortices because of the very small vortex-phonon scattering cross section; and second sound can no longer be propagated owing to the long mean free paths (for large angle scattering) of the excitations. A possible approach might involve measuring field emission and ionization characteristics in dilute ^{3}He–^{4}He solutions, since the controlled addition of further isotopic impurities would have the effect of adjusting F_2 in a manner which, in principle, would be amenable to calculation.

5. Conclusions

Although the field emission and field ionization currents in liquid helium vary in a complicated way with temperature and pressure, as well as with emitter potential, we have been able to account for most features of the observed phenomena in terms of existing knowledge of the liquid. We have not succeeded in developing a detailed explanation of the characteristics below 0.7 K, but we have inferred from our measurements that Vinen's F_2 parameter is almost independent of temperature in this range. A careful analysis of the experimental data has enabled us to deduce values of the ionic mobilities, and of the vortex nucleation and escape probabilities of negative ions; and, where comparisons were possible, we have found these values to be in reasonable agreement with those obtained in other experiments.

It is a pleasure to express our gratitude to colleagues for their help in diverse ways during the course of this work. In particular we are grateful to Dr H. Montagu-Pollock for technical advice and for many useful discussions, to Dr A. R. Birks for in valuable assistance with computing, to Mr N. Bewley who constructed the cryostat and experimental chamber, to Mr D. H. Bidle for much advice and assistance in connection with the ancillary electronic equipment, and to Mr S. S. Swarbrick for help in building the gas handling system. The research was supported (under contracts BSR 9251 and BRG 6094.8) by the Science Research Council to whom one of us (A. P.) is also indebted for the assistance of a studentship.

References

Abramowitz, M. & Stegun, I. A. 1965 (ed). *Handbook of mathematical functions*, pp. 260, 941, 978–983. New York: Dover.
Atkins, K. R. 1959 *Phys. Rev.* **116**, 1339.
Blaisse, B. S., Goldschvartz, J. M. & Slagter, P. C. 1970 *Cryogenics* **10**, 163.
Bruschi, L., Maraviglia, B. & Mazzoldi, P. 1966 *Phys. Rev.* **143**, 84.
Bruschi, L., Mazzoldi, P. & Santini, M. 1968 *Phys. Rev. Lett.* **21**, 1738.
Cade, A. G. 1965 *Phys. Rev. Lett.* **15**, 238.
Donnelly, R. J. 1967 *Experimental superfluidity*. Chicago and London: University of Chicago Press.
Donnelly, R. J. & Roberts, P. H. 1969 *Proc. R. Soc. Lond.* A **312**, 519.
Donnelly, R. J. & Roberts, P. H. 1971 *Phil. Trans. R. Soc. Lond.* A **271**, 41.
Gavin, P. J. & McClintock, P. V. E. 1973 *Phys. Lett.* **43** A, 257.
Gomer, R. 1961 *Field emission and field ionization: Harvard monographs in applied science no.* 9. Cambridge, Massachusetts: Harvard University Press.
Halpern, B. & Gomer, R. 1965 *J. chem. Phys.* **43**, 1069.

PHILOSOPHICAL TRANSACTIONS OF THE ROYAL SOCIETY A MATHEMATICAL, PHYSICAL & ENGINEERING SCIENCES

Halpern, B. & Gomer, R. 1969*a* *J. chem. Phys.* **51**, 1031.
Halpern, B. & Gomer, R. 1969 *b* *J. chem. Phys.* **51**, 1048.
Henson, B. L. 1970 *Phys. Lett.* **33**A, 91.
Hickson, A. 1971 M.Sc. dissertation, University of Lancaster (unpublished).
Hickson, A. & McClintock, P. V. E. 1970 *Proc. 12th Int. Conf. on Low Temperature Phys.* (ed. E. Kanda), p. 95. Tokyo: Keigaku Publishing Co.
Hickson, A. & McClintock, P. V. E. 1971 *Phys. Lett.* **34** A, 424.
Ihas, G. G. 1971 Ph.D. dissertation, University of Michigan, Ann Arbor (unpublished).
Ihas, G. G. & Sanders, T. M. 1970 *Phys. Lett.* **31**A, 502.
Ihas, G. G. & Sanders, T. M. 1971 *Phys. Rev. Lett.* **27**, 383.
McClintock, P. V. E. 1969 *Phys. Lett.* **29** A, 453.
McClintock, P. V. E. 1970 *Proc. 12th Int. Conf. on Low Temperature Phys.* (ed. E. Kanda), p. 101. Tokyo: Keigaku Publishing Co.
McClintock, P. V. E. 1971 *Phys. Lett.* **35**A, 211.
McClintock, P. V. E. 1972 *Proc. 13th Int. Conf. on Low Temperature Phys.* (ed. K. D. Timmerhaus, W. J. O'Sullivan and E. F. Hammel), vol. 1, p. 434. New York: Plenum Press.
McClintock, P. V. E. 1973*a* *J. Low Temp. Phys.* **11**, 15.
McClintock, P. V. E. 1973*b* *J. Low Temp. Phys.* **11**, 277.
McClintock, P. V. E. 1973*c* *J. Phys.* C **6**, L 186.
McClintock, P. V. E. & Read-Forrest, H. 1973 *Cryogenics* **13**, 371.
McClintock, P. V. E., Crowley, S. D. & Davis, P. J. 1973 *Cryogenics* **13**, 556.
Meyer, L. & Reif, F. 1961 *Phys. Rev.* **123**, 727.
Müller, E. W. & Tsong, T. T. 1969 *Field ion microscopy: principles and applications.* New York: American Elsevier.
Neeper, D. A. 1968 *Phys. Rev. Lett.* **21**, 274.
Neeper, D. A. & Meyer, L. 1969 *Phys. Rev.* **182**, 223.
Onn, D. G. & Silver, M. 1969 *Phys. Rev.* **183**, 295.
Padmore, T. C. 1972*a* *Phys. Rev.* A **5**, 356.
Padmore, T. C. 1972*b* *Phys. Rev. Lett.* **28**, 469.
Parks, P. E. & Donnelly, R. J. 1966 *Phys. Rev. Lett.* **16**, 45.
Phillips, A. & McClintock, P. V. E. 1973 *Phys. Lett.* **46**A, 109.
Phillips, A. & McClintock, P. V. E. 1974 *J. Phys.* C **7**, L 118.
Rayfield, G. W. 1966 *Phys. Rev. Lett.* **16**, 934.
Rayfield, G. W. 1968 *Phys. Rev.* **168**, 222.
Rayfield, G. W. & Reif, F. 1964 *Phys. Rev.* **136**, A 1194.
Reichert, J. F. & Dahm, A. J. 1974 *Phys. Rev. Lett.* **32**, 271.
Schwarz, K. W. 1972 *Phys. Rev.* A **6**, 837.
Sitton, D. M. & Moss, F. 1971 *Phys. Lett.* **34**A, 159.
Sitton, D. M. & Moss, F. 1972 *Phys. Rev. Lett.* **29**, 542.
Springett, B. E. & Donnelly, R. J. 1966 *Phys. Rev. Lett.* **17**, 364.
Takken, E. H. 1970 *Phys. Rev.* A **1**, 1220.
Vinen, W. F. 1957 *Proc. R. Soc. Lond.* A **242**, 493.
Vinen, W. F. 1958 *Proc. R. Soc. Lond.* A **243**, 400.
Zoll, R. & Schwarz, K. W. 1973 *Phys. Rev. Lett.* **31**, 1440.

Note added in proof, 2 *January* 1975.

Contrary to Takken's (1970) theoretical prediction, a very recent experimental investigation (A. Phillips and P. V. E. McClintock, *Phys. Rev. Lett.* **33**, 1468 (1974)) has shown that under electric fields of a few hundred V mm^{-1} the drift velocity of negative ions exceeds v_L by ca. 30 % for $T < 0.5$ K. The arguments of § 4*d* still stand, however, although the average values deduced for ν (figure 26) may accordingly be ca. 30 % too small. In addition, the apparent negative dependence of ν on F in figure 26*a* has been confirmed.

PHILOSOPHICAL TRANSACTIONS OF THE ROYAL SOCIETY A MATHEMATICAL, PHYSICAL & ENGINEERING SCIENCES